Wind-Driven Transport Fluctuations through Drake Passage: A Southern Mode

CHRIS W. HUGHES

Proudman Oceanographic Laboratory, Bidston Observatory, Birkenhead, Merseyside, United Kingdom

MIKE P. MEREDITH AND KAREN J. HEYWOOD

School of Environmental Sciences, University of East Anglia, Norwich, United Kingdom

(Manuscript received 31 March 1997, in final form 3 August 1998)

ABSTRACT

It is proposed that, for periods between about 10 and 220 days, the variability in Antarctic circumpolar transport is dominated by a barotropic mode that follows f/H contours almost everywhere. Theoretical arguments are given that suggest the possible importance of this mode and show that bottom pressure to the south of the current should be a good monitor of its transport. The relevance of these arguments to eddy-resolving models is confirmed by data from the Fine Resolution Antarctic Model and the Parallel Ocean Climate Model. The models also show that it may be impossible to distinguish the large-scale barotropic variability from local baroclinic processes, given only local measurements, although this is not generally a problem to the south of the Antarctic Circumpolar Current. Comparison of bottom pressures measured in Drake Passage and subsurface pressure on the Antarctic coast, with wind stresses derived from meteorological analyses, gives results consistent with the models, showing that wind stress to the south of Drake Passage can explain most of the observed coherence between wind stresses and circumpolar transport. There is an exception to this in a narrow band of periods near 20 days for which winds farther north seem important. It is suggested that this may be due to a sensitivity of the ''almost free'' mode to winds at particular locations, where the current crosses f/H contours.

1. Introduction

Since November 1988, as part of the Antarctic Circumpolar Current Levels from Altimetry and Island Measurements (ACCLAIM) project (Spencer et al. 1993), the Proudman Oceanographic Laboratory (POL) has been deploying bottom pressure recorders (BPRs) on either side of Drake Passage, as a contribution to the World Ocean Circulation Experiment choke point monitoring. Instruments have been deployed in three different north–south configurations close to Drake Passage, each deployment lasting approximately one year. The positions and times are summarized in Fig. 1 and Table 1. This is not a complete list of deployments in the area, which also include positions at intermediate latitudes (Spencer and Vassie 1997; Meredith 1995).

The intention was to use the BPRs to monitor transport in the Antarctic Circumpolar Current (ACC) to help establish the dynamics of ACC transport fluctuations and, in conjunction with measurements by other groups at choke points south of Africa and Australia, to assess the zonal coherence of those fluctuations. The purpose of this paper is to investigate how well the transport fluctuations can be measured by BPRs and to look for a relationship between the transport and the wind stress over the Southern Ocean. This follows on from the International Southern Ocean Studies (ISOS) experiment, conducted in the mid-1970s and early 1980s, which established that much of the transport variability was reflected by the bottom pressure (Whitworth 1983; Whitworth and Peterson 1985) and that the transport fluctuations are related to the wind field (Wearn and Baker 1980; Chelton 1982; Peterson 1988a).

The next section of this paper revisits the theory of wind-driven fluctuations in the transport through Drake Passage, and the following section considers the problem of relating bottom pressure measurements to transport fluctuations. These theoretical remarks are then tested by recourse to data from the Fine Resolution Antarctic Model (FRAM), an eddy-permitting model of the Southern Ocean, where it is shown that the concept of barotropic fluctuations is only relevant to large-scale currents or regions to the south of the ACC. The new BPR data are then compared with wind stresses from meteorological analyses, and the results of this comparison are discussed in the light of theory, model, and ISOS results. The picture that has been built up is then

Corresponding author address: Dr. Chris W. Hughes, Proudman Oceanographic Laboratory, Bidston Observatory, Birkenhead, Merseyside L43 7RA, United Kingdom.
E-mail: c.hughes@pol.ac.uk

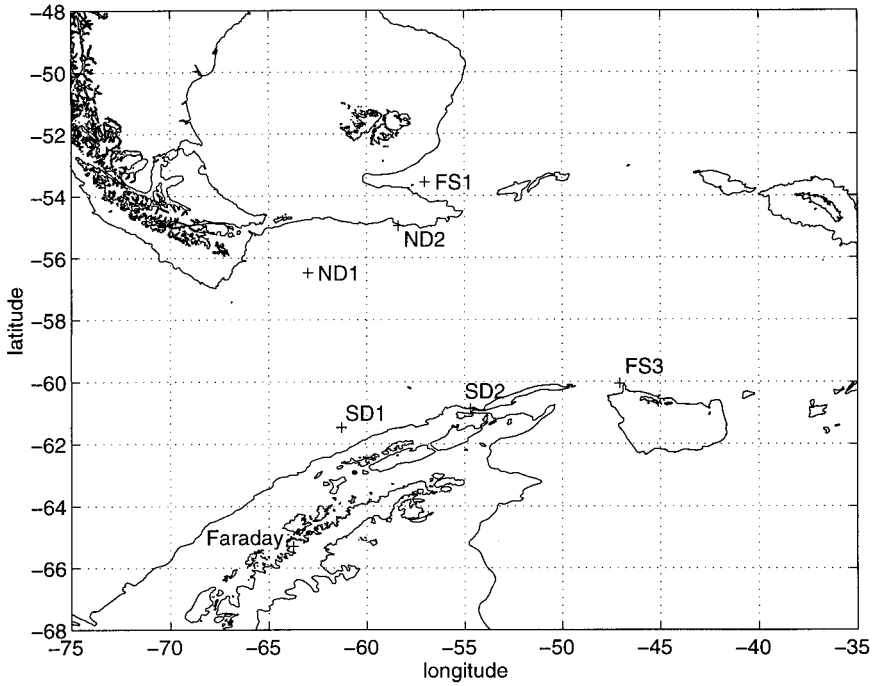

FIG. 1. Map of the Drake Passage area showing the positions of BPRs discussed in this paper, and of the Faraday tide gauge. Also shown are the coastline and the 1000-m depth contour.

tested further using model data from the Parallel Ocean Climate Model (POCM), a global model with more realistic wind stress forcing.

2. Dynamics of ACC transport

a. The mean flow

The dynamics of the ACC are unique because of the lack of meridional barriers at the latitudes of Drake Passage. Munk and Palmén (1951) were the first to point out that this means that bottom topography must be important in balancing the eastward wind stress at these latitudes. In a closed basin, the angular momentum input due to a zonal mean wind stress can be balanced by a pressure difference across the basin, producing a torque on the solid earth via the continental boundaries. If there are no boundaries, the torque must be produced by another mechanism. The transports that would be necessary to allow horizontal friction or transient eddy processes to carry angular momentum to the blocked latitudes are much larger than those observed, unless very large eddy friction coefficients are assumed. Similarly, vertical eddy transport is inadequate in the flat bottom case. A relatively small pressure difference of a few centimeters of water across the major topographic features of the Southern Ocean is, however, quite adequate to balance the input by wind stress.

Stommel (1957) pointed out that there is no latitude for which the minimum depth is greater than about 1000 m. He therefore decided on a model in which the Southern Ocean is closed at all latitudes but has a zonal gap between South America and the Antarctic Peninsula/Scotia arc region. Effectively, he was assuming that the topography penetrates close enough to the surface to act as a continent. He then invoked a conventional (flat bottom, or no interaction with topography) Sverdrup balance at latitudes north of Drake Passage, but with a zonal jet to close the circulation. This zonal jet appears because south of Drake Passage he assumed an unconventional Sverdrup balance in which the streamfunction is calculated by integrating wind stress curl eastward from the western boundary, instead of westward from the eastern boundary. There is no very good reason for

TABLE 1. Details of deployments of ACCLAIM bottom pressure recorders at northern and southern extremes of Drake Passage.

Site	Start	End	Latitude (°S)	Longitude (°W)	Depth (m)
FS1	27 Nov 88	11 Nov 89	53.540	57.015	2803
FS1	11 Nov 89	21 Nov 90	53.539	57.031	2800
FS1	21 Nov 90	09 Jan 92	53.512	56.980	2800
FS1	12 Jan 92	21 Jul 92	53.523	57.032	2800
ND1	22 Dec 91	06 Nov 92	56.491	52.985	3925
ND2	09 Nov 92	22 Nov 93	54.942	58.393	1010
ND2	22 Nov 93	15 Nov 94	54.943	58.392	1007
FS3	14 Nov 89	24 Nov 90	60.037	47.100	2180
FS3	23 Nov 90	07 Jan 92	60.052	47.085	2010
FS3	07 Jan 92	23 Nov 92	60.052	47.167	2267
SD1	23 Dec 91	07 Nov 92	61.474	61.291	3946
SD2	13 Nov 92	26 Nov 93	60.850	54.715	1020
SD2	27 Nov 93	21 Nov 94	60.850	54.714	1020

doing this, as Stommel was aware, pointing out that these remarks ''cannot be considered to be a theory; they are merely suggestive of one.'' By this reasoning, the strength of the ACC is determined by the southward transport due to nontopographic Sverdrup balance at the northernmost latitude of Drake Passage, and hence by the zonally integrated wind-stress curl at that latitude.

Baker (1982) used the Han and Lee (1981) winds to calculate this Sverdrup transport across 55°S and derived a value of 190 ± 60 Sv (Sv ≡ 10^6 m^3 s^{-1}), comparable with the contemporary estimate of 127 ± 12 Sv for transport through Drake Passage, by Whitworth et al. (1982). The zonal distribution of the implied southward return flow is also similar to that inferred (for the baroclinic flow) from hydrography, with most of the southward motion occurring in the Indian Ocean sector where the wind stress curl is strongest. There is support for these conclusions from calculations using the Hellerman and Rosenstein (1983) wind climatology (Chelton et al. 1990), and in FRAM, too, Wells and de Cuevas (1995) find that the net southward transport across 55°S, away from the Falklands Current, is close to an integrated nontopographic Sverdrup balance with the wind stress curl (although this does not make up the complete flow through Drake Passage). So the empirical basis for the significance of Sverdrup-type dynamics seems quite persuasive. However, the question of how nontopographic Sverdrup dynamics can persist in a region where interactions with bottom topography are necessary is yet to be explained. A zonal jet, shallower than 1000 m, confined to the Drake Passage latitudes, can be added to the Sverdrup-type solution without altering the meridional currents, which are all that is specified by Sverdrup balance. In this sense, the Sverdrup solution still cannot be considered an explanation of the strength of the ACC until a reason is given for selection of a strength for the zonal jet. For more discussion of this matter, see Warren et al. (1996, 1997), Hughes (1997), and Olbers (1998).

Another model for the mean ACC is that of Gill (1968) in which flat-bottomed Sverdrup regimes to the north and south of Drake Passage, and a zonal jet in Drake Passage, are connected by frictional boundary layers. Again, a reasonable shape for the ACC is obtained, with a sharp northward deflection east of Drake Passage, and gradual southward return elsewhere. The lack of bottom topography still means that high friction coefficients are necessary to limit the transport to reasonable values. Gill recommended lateral friction of 10^4 m^2 s^{-1}, or vertical friction of 10^{-1} m^2 s^{-1}. With such high friction, the zonal jet is reduced to carrying only 25% to 40% of the ACC transport, and the Sverdrup balance is significantly modified by friction almost everywhere. A very similar solution was produced by Klinck (1991). These values of friction are within the range typically used as a parameterization of mesoscale eddies, but it has been shown (Morrow et al. 1994; Bryden and Heath 1985) that eddies in the real ocean do not produce Reynolds stresses strong enough to balance the winds in this way. Lateral frictions in eddy-resolving models are typically less than 200 m^2 s^{-1}.

Given that eddies and friction are too small to balance the wind stress, bottom topography must be important. Johnson and Bryden (1989) proposed that eddies could provide the mechanism whereby angular momentum input by wind stress is transferred to depths where the flow can interact with topography; however, numerical model results (Treguier and McWilliams 1990; Wolff et al. 1991; Killworth and Nanneh 1994) suggest that it is the time average flow, rather than transient eddies, that produces most of the form stress.

b. Fluctuations in the flow

The above models are all of the mean flow in the ACC and are described because they form an important background to many investigations into the time variability of the ACC. However, it will be seen that the dynamical nature of the transport variability is, in fact, profoundly different from that of the mean flow. Most authors agree that, for periods less than about a year, fluctuations in ACC transport are mostly barotropic (the term is used throughout this paper to mean a flow that has a geostrophic component—and thus a horizontal pressure gradient—independent of depth. Thus, a wind-driven barotropic flow consists of an Ekman flow, a depth-independent geostrophic flow, and possibly other ageostrophic components). Support for this view comes from the analytical and modeling study by Willebrand et al. (1980) (although this study was aimed at the mid-latitudes), the analytical solution by Clarke (1982) based on a similarity solution of the time-dependent thermocline equations for a flat bottom, and measurements in Drake Passage reported by Whitworth and Peterson (1985). Strong evidence for barotropic pressure fluctuations at the south side of Drake Passage is given by Peterson (1988a) and Meredith et al. (1996). Physically, the reason for this is that the barotropic response to wind stress is mediated by relatively fast-moving barotropic topographic Rossby waves, or ordinary barotropic Rossby waves in the flat bottom case (Anderson and Gill 1975; Anderson and Killworth 1977; Hughes 1996). Wearn and Baker (1980) refer to the even faster long gravity waves, which can travel around Antarctica in approximately one day. The role of gravity waves on longer timescales can be seen as setting up the surface elevation consistent with near-geostrophic dynamics. On the timescale of barotropic gravity waves, divergence is important, so there can be a significant net transport into a closed region, making the definition of transport around Antarctica a highly localized one. For this reason, the analysis here concentrates on longer timescales, greater than about 10 days.

Baroclinic Rossby waves move much more slowly, especially at high latitudes. In fact, within the ACC there is evidence that the mean current is strong enough to

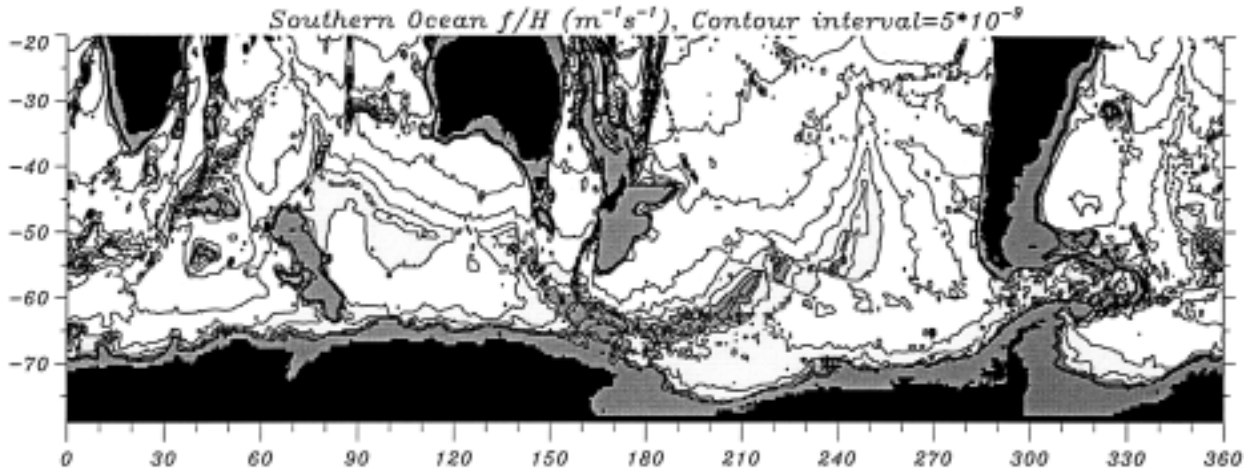

FIG. 2. Contours of f/H in the Southern Ocean, from the DBDB5 topography averaged onto a half-degree grid, plotted with a contour interval of 5×10^{-9} m^{-1} s^{-1}. The minimum value is -5×10^{-8} m^{-1} s^{-1}, and light gray shading is between -4 and -3×10^{-8} m^{-1} s^{-1}, or H/f values between -2.5 and -3.333×10^{7} s m.

advect baroclinic waves eastward (Hughes et al. 1998), so the baroclinic response is limited to much smaller length scales. It should however be noted that much of the ACC transport is concentrated in narrow jets with a strong eddy field, so it cannot be taken for granted that there is no baroclinic response on these length scales. For example, Meredith et al. (1996, 1997) give very convincing evidence that fluctuations on small length scales (less than 200 km) can dominate the bottom pressure record at certain locations, making such records useless as a monitor of the large-scale flow. Since the net transport must be a large-scale flow (it has to be coherent around large fractions of Antarctica), we will assume that the dynamics of wind-driven transport fluctuations are barotropic for periods shorter than a year. This is an assumption that is almost certainly not entirely valid since the interaction of wind stress with narrow, intense, baroclinic jets is a complicated matter, which may also produce transport fluctuations. However, the simplification permits a more detailed explanation of this aspect of the dynamics that produces a useful framework within which the observations and model results may be examined. Even assuming a barotropic response on the large scale does not guarantee that this response will be detectable in local measurements, as the signal at any one place may be dominated by baroclinic fluctuations at small scales.

As Willebrand et al. (1980) pointed out, for a barotropic response it is vitally important to take account of the bottom topography. The characteristics along which barotropic Rossby waves propagate are not lines of constant latitude, but lines of constant f/H, where f is the Coriolis parameter and H the ocean depth. At midlatitudes, gradients of f/H are dominated by variations in H if the slope is large enough to produce an order-1 difference in ocean depth over horizontal distances less than one earth radius. At high latitudes, topography becomes relatively more important as beta (the meridional gradient of f) decreases. Throughout the Southern Ocean, the variation of f/H is dominated by topographic effects (Fig. 2). For barotropic fluctuations then, any Sverdrup balance must be a topographic Sverdrup balance in which the effective western boundary is determined in relation to the gradient of f/H rather than f. The Sverdrup balance is set up by the propagation of topographic Rossby waves, with typical propagation speeds of several meters per second. Willebrand et al. (1980) estimate that a flat-bottom Sverdrup balance would take about 30 days to come into equilibrium at midlatitudes. At higher latitudes beta is smaller, but the effective beta is dominated by topography, so 30 days is probably an upper limit on the time needed for Sverdrup balance to be set up on the largest scales, and a typical value for the smaller scales characteristic of the bottom topography (except where closed contours of f/H do not allow a barotropic Sverdrup balance to be established).

Clarke (1982) applies flat-bottom barotropic dynamics to ACC fluctuations, although he attempts to include topographic effects by employing a large drag to represent topographic form stress. Wearn and Baker (1980) assume a similar model to that derived by Clarke (1982), in which a zonal jet is accelerated by winds and retarded by friction (or form drag) with a time constant, based on correlations between zonal average winds and measured bottom pressure difference across Drake Passage, of between 5.5 and 9.5 days. The models implicit in Peterson (1988a) also use flat bottom dynamics, concentrating on the importance of zonally averaged wind stress over the ACC region, and wind stress curl north and south of this region, although in this case the models were simply used as scenarios to compare with observations, without advocating the use of flat bottom dynamics (indeed, it was concluded that other dynamics

must be involved). None of these models take adequate account of the dramatic change in barotropic dynamics when topography is included. This change is illustrated by the results of Klinck (1991) in which the mean transport of a barotropic ACC drops from 180 Sv without topography (but with large friction, with a spindown time of less than 6 days) to 10–25 Sv with topography. The reason for this, as explained below, is probably that there is a much smaller cross-sectional area over the region of f/H contours that pass around Antarctica than the area of the whole Drake Passage region without bottom topography. This result emphasizes that barotropic dynamics, which can reasonably be applied to relatively short period fluctuations, produce quite different results from either the flat-bottom case or the baroclinic case with topography, which is needed to explain the mean flow.

If the linear momentum equations are integrated over the depth of the ocean, the result can be written as

$$\rho_0 \mathbf{k} \times \nabla \Psi_t - \rho_0 f \nabla \Psi = -H \nabla p_b - \nabla E + \boldsymbol{\tau}, \quad (1)$$

where Ψ is the vertically integrated streamfunction (the rigid-lid approximation has been made, and subscript t represents differentiation with respect to time), H is depth, ρ_0 is a reference density, p_b is the bottom pressure, $\boldsymbol{\tau}$ the surface wind stress (it can also be taken to include the other neglected quantities), and E is potential energy,

$$E = g \int_{-H}^{0} z\rho \, dz, \quad (2)$$

measured relative to the surface. Dividing by H and then taking the curl gives

$$\nabla \cdot \left(\frac{\nabla \Psi_t}{H} \right) + \rho_0 J(\Psi, f/H) = J(E, 1/H) + \mathbf{k} \cdot \nabla \times \frac{\boldsymbol{\tau}}{H}. \quad (3)$$

If H is set to a constant, this reduces to the conventional Sverdrup balance in the steady state. With variable bottom topography, the first term on the right-hand side represents the effect of stratification. Although this is very important in the time mean flow, providing a mechanism that insulates the flow from effects of the bottom topography, it is less important at seasonal timescales and large length scales. This was demonstrated by Gill and Niiler (1973) who considered barotropic dynamics assuming length scales of 3000 km zonally and 1000 km meridionally, driven by seasonal winds. They concluded that time dependence of E due to density advection by the resulting flow produces a negligible perturbation to the assumed flow, showing that it is self-consistent to take E as constant over these timescales. Although the assumed length scales are rather large, the effect of density advection is particularly small at high latitudes so that, at around 60°S, this scaling would still apply over length scales reduced by a factor of 10 [see Eq. (8.5) and following comments in Gill and Niiler (1973)]. Of course, E can also change as a consequence of convection-driven flows, and this might be expected to be a significant process close to Antarctica, especially at the annual period. It can also change because of advection of small-scale features such as intense jets (for which the linear vorticity dynamics assumed by Gill and Niiler would be inappropriate) but, for the purposes of this investigation, we are assuming that these processes do not dominate the dynamics.

The remaining balance of terms is between a time-dependent term that permits topographic Rossby waves (and can be ignored in most regions once the Sverdrup balance has been set up), the flow across contours of f/H, and the curl of $\boldsymbol{\tau}/H$, so water can get through Drake Passage by means of a forced flow across f/H contours. At first glance, it might seem that this forced flow would be smaller than the flat bottom equivalent, since gradients of f/H, suitably normalized, are larger than beta, but in fact the two are exactly the same in an integrated sense. As pointed out by Hughes and Killworth (1995), if (1) is integrated around a closed contour of H (ignoring time dependence), then the effects of stratification and bottom topography both drop out, leaving

$$-\rho_0 \oint_{\substack{\text{const} \\ H}} f \nabla \Psi \cdot d\mathbf{s} = \oint_{\substack{\text{const} \\ H}} \boldsymbol{\tau} \cdot d\mathbf{s}. \quad (4)$$

Applying Stokes theorem then gives

$$\rho_0 \int_{\substack{\text{const} \\ H}} \beta \Psi_x \, dS = \rho_0 \int_{\substack{\text{const} \\ H}} \nabla \times \boldsymbol{\tau} \, dS, \quad (5)$$

which is the Sverdrup balance integrated over the enclosed area (the physical reason for this balance is that the bottom pressure torque vanishes over areas enclosed by contours of constant depth). This could be the basis for a relationship between wind stress curl and ACC transport, although it is clearly not the curl along a particular latitude that is important; frictional effects may be relevant (especially near the coast), and the relationship between the meridional transport in (5) and the zonal transport through Drake Passage is far from transparent. Although time dependence has been ignored, this argument would also apply to variations in the topographic Sverdrup mode on timescales long enough for this mode to come into equilibrium since the time-dependent term is much smaller than the other terms in this situation.

The actual ACC transport produced by the forced flow is difficult to calculate because of the complicated shape of the f/H contours, but there is another component that should be considered too. There are contours of f/H that pass all the way around Antarctica (dark shading in Fig. 2). Any flow along these contours needs no curl of $\boldsymbol{\tau}/H$ to drive it. In the linear, unstratified case, the flow along such contours cannot come into a Sverdrup balance and will (as shown below) continue to accelerate until either the forcing reverses or a frictional balance is attained.

Being unconstrained by the topographic Sverdrup balance, this is often called a (linear) ''free'' mode (Read et al. 1986; Branstator and Opsteegh 1989), analogous to a purely zonal flow in the flat bottom case (the flow is free in the sense that, in the absence of stratification and viscosity, it could persist indefinitely without forcing, unlike the mode forced by curl of $\boldsymbol{\tau}/H$). For forcing with a period longer than the Sverdrup spinup time, this is therefore the mode that comes to dominate the solution, unless stratification comes to balance the forcing.

Integrating (1) around a closed contour of f/H, dropping the effect of stratification, gives

$$\rho_0 \oint_{f/H} \overline{\mathbf{u}}_t \cdot d\mathbf{s} = \oint_{f/H} \frac{\boldsymbol{\tau}}{H} \cdot d\mathbf{s}, \tag{6}$$

where $\overline{\mathbf{u}} = \mathbf{k} \times \nabla\Psi/H$. Here, the line integral of wind stress produces an accelerating flow [not necessarily following the f/H contour, it is only the integral acceleration that is specified by (6), although for periods much longer than the topographic Rossby wave period all flows across f/H contours must be proportional to the wind stress rather than its time integral, leaving the accelerating flow to follow the f/H contour in this limit], in contrast to the Sverdrup balance case where the curl produces a steady flow. In reality, of course, the acceleration will be halted, either by some kind of (eddy) friction or by a feedback from density advection on the value of E in (3); so for times longer than the frictional (or advection) time constant the flow will follow the wind stress, with a time lag. The free flow thus obeys dynamics rather like the frictional zonal jet assumed by Clarke (1982) and Wearn and Baker (1980), but topography has been taken into account; and a higher effective friction is no longer due to larger-scale topographic effects, which need not act as a drag at all, but to the narrow, convoluted path of the current and to small-scale topographic drag or effects of stratification.

The distinction between Sverdrup and free flow can be made more formally (Hughes 1995), especially where the boundary follows contours of f/H, which could reasonably be considered to be the case here. The inviscid formula for the free flow component is

$$\rho_0 \frac{\partial}{\partial t} \frac{\partial \Psi_0}{\partial \dfrac{f}{H}} \oint \frac{\left|\nabla \dfrac{f}{H}\right|}{H} ds = \oint \frac{\boldsymbol{\tau}}{H} \cdot d\mathbf{s}, \tag{7}$$

where $\Psi_0 = \Psi_0(f/H, t)$ is the free mode component of the streamfunction. Even without friction it is difficult to work out the size of the response, because of the complicated form of the integrals involved and their sensitive dependence on the shape of depth contours. One thing is clear though: the free mode response is driven by wind stress (not curl), averaged along lines that fall mostly on the southern side of Drake Passage.

It should be stressed that both the free mode and the Sverdrup response are capable of producing circulation around Antarctica, and the two are quite closely related. The topographic Sverdrup balance gives the component of flow across f/H contours, and the component along f/H contours is then inferred by mass continuity (except that this is insufficient for f/H contours that are closed). Thus, close to the closed f/H contours around Antarctica there are contours of f/H, that almost close around the continent, and the flow along these contours will be very sensitive to the Sverdrup transport across f/H contours. A simple example would be a wind field that produces Sverdrup transport to larger (negative) values of f/H (i.e., toward the unblocked f/H contours in shallower regions near Antarctica) to the west of Drake Passage, and the opposite way east of Drake Passage. The water could then flow through Drake Passage along unblocked f/H contours and continue eastward around Antarctica in the deeper region of f/H contours, which are blocked only in Drake Passage. Alternatively, the flow on unblocked contours might not pass through Drake Passage but could return the ''long way around'' in a westward current. The difference between these two cases is the behavior of the free mode. Thus, the free mode also makes possible an ''almost free mode,'' in which transport is along f/H contours almost everywhere, but skips across contours at certain places.

The dynamics involved is illuminated by considering the role of the Ekman transport. Assuming a timescale longer than that of topographic Rossby wave, so that the time-dependent term may be dropped from (1), and taking the stratification to be constant in time, divide (1) by f and take the curl, then subtract the time average to give

$$J(p_b', H/f) = -\mathbf{k} \cdot \nabla \times \frac{\boldsymbol{\tau}'}{f}, \tag{8}$$

where the prime denotes deviations from the time average. The right-hand side of (8) is the convergence of the Ekman transport, and the left-hand side is the divergence of the depth-integrated geostrophic flow. Thus we see that a geostrophic flow follows H/f contours except where the depth-integrated geostrophic flow becomes convergent in order to feed a divergent Ekman transport (or vice versa). The importance of the free mode becomes apparent if (8) is integrated over an area bounded by a closed contour of H/f. The left-hand side then vanishes, leaving the Ekman transport into the region unbalanced. In order to balance this transport, one of the terms that was ignored in (1) must be reinstated. Initially, the most important will be the acceleration, producing an accelerating circulation around closed f/H contours until either friction or stratification become important. However, a pure free mode will not generally occur. Since the divergence of the Ekman transport will not generally be constant along the closed H/f contours, it will vary, producing a flow across contours. The average divergence of Ekman transport along an H/f con-

tour is balanced by the time-dependent term, but the difference from that average will produce flows across H/f contours of both signs, integrating to zero and linking the free mode flow to flow along nearby H/f contours. Thus, an almost free mode is produced. Whether the free or the almost free mode is the more important depends on the geometry, the form of the wind stress forcing, and the time it takes for the free mode to reach a steady state, and is difficult to assess analytically.

The third possibility is that transport can occur due to a forced mode that is not closely related to the free mode. If such a mode is to pass right around Antarctica without making use of those f/H contours that pass most of the way around the continent, it would require a complex series of transports across f/H contours, alternating between passing to higher and then lower values several times along the circuit. Again, the likely size of this component is difficult to assess analytically, but it seems reasonable to predict that it would be smaller than the free or nearly free modes, which rely on a wind stress aligned with the mostly zonal closed H/f contours.

The essentials of the argument can be summarized as follows: it is much easier to produce a barotropic flow along f/H contours than across contours. The component of the flow that encircles Antarctica is therefore likely to follow those f/H contours that encircle, or almost encircle, the continent.

The shaded region in Fig. 2 is an attempt to show the zone that might be expected to play a part in the free and almost free modes. Dark shading represents values of f/H that, at the south side, go all the way around Antarctica, although almost all of this area is at depths less than 1000 m. The lighter shading is for contours that are only interrupted by small-scale features at Drake Passage. The smallest scales will certainly be irrelevant here, since nonlinear effects can effectively smooth out the f/H contours. The scale over which this smoothing is effective depends on the strength of the current, and the mean flow in Drake Passage is very strong. An estimate of the smoothing effect can be made by comparing vorticities u/L and $f\delta H/H$, where L is the length scale to be smoothed out. Assuming a $\delta H/H$ of 0.1, a 1 ms^{-1} mean current could smooth such a feature over a distance of about 100 km.

This picture of the barotropic response to winds demonstrates that it makes little sense to think of wind-driven fluctuations as changes in the strength of the mean flow, for timescales shorter than a year. Any barotropic fluctuations in transport must be strongly topographically controlled (much more so than the path of the mean flow) and consist of a free mode and a Sverdrup response that bear little relation to the mean flow (and probably also some response in the narrow jets of the ACC, neglected here). Thus the transient current flows across streamlines of the mean flow. This need not produce strong interactions with the mean flow if the fluctuating current does not significantly displace the mean current. A fluctuating current, with period 1 yr and amplitude 2 cm s^{-1}, produces a peak displacement of about 100 km, small on the scale of the ACC.

3. Theory of measurement

From 1976 to 1981, as part of the ISOS program, BPRs were deployed across Drake Passage at about 500-m depth in an attempt to monitor the transport of the ACC (Wearn and Baker 1980; Whitworth 1983; Whitworth and Peterson 1985; Peterson 1988a). In 1979, a year-long deployment of moored current meters and temperature sensors was undertaken along a transect crossing the BPRs, and data from this year were used to show that the majority of the transport variability for periods shorter than a year is barotropic, and to give a calibration relating pressure differences across Drake Passage to the net transport above 2500 m (Whitworth and Peterson 1985).

For barotropic variations, the transport variation between two points depends not only on the pressure difference variations, but also on the value of f/H where the current flows. The total transport is

$$T = \int_a^b \int_{-H}^0 u \, dz \, ds = \int_a^b H u_g \, ds + T_{\mathrm{Ek}}, \qquad (9)$$

where u_g is the geostrophic velocity perpendicular to the section between horizontal positions a and b, and T_{Ek} is the transport across this section in the Ekman layer (plus any other ageostrophic flow that may occur). Geostrophy gives $\rho_0 f u_g = \partial p/\partial s$, so

$$T_g = \int_a^b \frac{H}{f\rho_0} \frac{\partial p}{\partial s} \, ds, \qquad (10)$$

where T_g is the geostrophic contribution to the transport.

If points a and b both lie on the same contour of f/H, then the path of integration can be taken along this contour, so H/f can be taken out of the integral giving

$$T_g = \frac{H}{f\rho_0}(p_b - p_a). \qquad (11)$$

When the points are not connected by a contour of f/H, this simplification is not possible and the relationship between transport and pressure depends on the path of the current, which might fluctuate over time. For a region as constricted as Drake Passage, the possible variation in f is quite small [1.22 to 1.27 ($\times 10^{-4}$ s^{-1}) for the ISOS BPRs], but with the BPRs at only 500-m depth, there is no section joining these two points that does not undergo a depth change of at least a factor of 2. The importance of this effect is demonstrated by the large difference found by Whitworth and Peterson (1985) when they attempted to correct their transport estimates for the effect of fluctuations in the currents on the shelf slope between the 500 m and 2500 m contours. Thus fluctuations in pressure difference between two points at the same depth, despite being a good measure of the fluctuations in the horizontally integrated

current (if the two points are at similar latitudes), need not be a good measure of the net transport fluctuations, integrated over depth as well as horizontally. They may instead represent movements of the current so that it flows with varying distributions of f/H values, even in the purely barotropic geostrophic case. For the Sverdrup component of the response to wind forcing, this can make observations difficult to interpret since this component is due to flow across f/H contours varying over time, so the current must be at different values of f/H at different times.

If the current is assumed to have a fixed path, or one for which the distribution over values of f/H does not vary significantly in time (implying that the current is either a free mode or a part of the Sverdrup response that is not forced locally—a description that applies well to the almost-free mode), then the relationship between transport and pressure difference can be used to infer an effective value of H/f:

$$\left(\frac{H}{f}\right)_e = \frac{T\rho_0}{(p_b - p_a)} = \frac{\int_a^b \frac{H}{f}\frac{\partial p}{\partial s}\, ds}{(p_b - p_a)}. \qquad (12)$$

For a very narrow geostrophic current, this reduces to the value of H/f at which the current flows. For broader currents it is a weighted average of the values of H/f at which significant pressure gradient exists.

Thus, implicit in the notion that bottom pressure differences are a monitor of transport fluctuations is the assumption that the current that produces those transport fluctuations flows with an effective f/H that does not vary in time. That assumption is related to the role of the Ekman layer transport, mentioned above. If the integral from a to b in (10) is taken along two different paths, with different Ekman fluxes across those paths, it becomes clear that T_g is a path-dependent quantity; it is only the total transport that is independent of path (ignoring changes in free surface height). This is a severe problem unless the geostrophic transport is much greater than the Ekman transport, and is therefore not determined by the local wind stress.

The above discussion concerns the relationship between volume transports and pressure differences but does not address how the fluctuations in pressure difference are apportioned between the two pressure measurements. The additional information that is needed is mass continuity. For the situation considered here the mass of water in the ocean is conserved so that, ignoring the variation of gravity with latitude, the global integral of bottom pressure must remain constant. The unforced free mode is the simplest to analyze in this respect since setting Ψ to a function of f/H tells us [from (1)] that p_b is a function of f/H. Thus, in going from no flow to a free mode flow, the bottom pressure on one side of the f/H contours must rise, and that on the other side must fall. Conservation of mass tells us that the size of the rise or fall must be in inverse proportion to the area on that side of the closed contours. The area south of the closed contours around Antarctica is so much smaller than the area to the north that we would expect almost all of the bottom pressure signal to be seen at the south.

For the Sverdrup mode things are more complicated since it is not so easy to see what bottom pressure distribution would arise; but it seems reasonable to assume that it would still be a change in bottom pressure across the current that has the same sign at all longitudes (at least for that part of the current that passes south of Africa, Australia, and South America), permitting a similar argument to be made. Certainly, the almost free mode must produce a bottom pressure field close to that of the free mode, so we would expect both free and almost free modes to be reflected much more strongly in bottom pressure at the southern side of Drake Passage than at the northern side.

4. Model results

A complete justification of the approximations made in the discussion above would require some very sophisticated scaling arguments. Some arguments have been given for large scales, on the assumption that interactions with smaller-scale processes are not dominant, but that assumption is hard to justify analytically. Instead, we will use a rather more sophisticated numerical model to test these scalings. The Fine Resolution Antarctic Model, which is used, has its limitations, but it is probably safe to say that the real ocean is at least as complicated as the model ocean. Any simplifying assumptions that do not hold in the model ocean are unlikely to hold in the real ocean. In this way we can at least make sure that our assumptions are consistent with a more complete dynamical system, closer to the real ocean.

FRAM (FRAM Group 1991) is a model of the Southern Ocean, south of 24°S, with a resolution of 0.25° in latitude by 0.5° in longitude and 32 vertical levels. The model was spun up by relaxation to Levitus (1982) temperature and salinity values. The data considered here are from six years of ''free running,'' in which relaxation to the Levitus climatology is only applied in the surface layer, as a crude approximation to climatological heat and freshwater fluxes. The wind stresses are monthly, linearly interpolated from the Hellerman and Rosenstein (1983) climatology. The topography is smoothed to about 1° resolution to avoid instabilities. Grose et al. (1995) give a good description of the strengths and weaknesses of the model in its representation of the mean flow in the Drake Passage region.

The dataset used comprises 72 monthly snapshots over the 6-yr free running period. Total volume transport is also available as a daily time series over almost seven years (Fig. 3). The transport variability can be decomposed into three parts: a long-term climate drift; an annually repeating signal, and a shorter period variability that does not tend to repeat from year to year. The long-

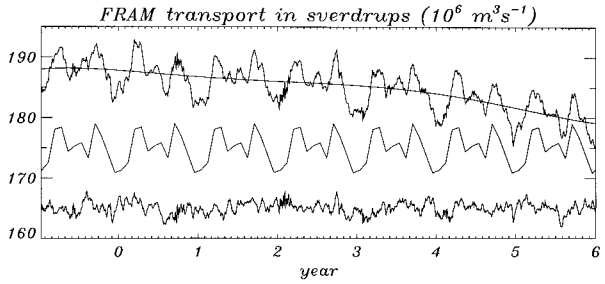

FIG. 3. Time series of Drake Passage transport from FRAM. The top curve shows the complete time series, with a polynomial fit superimposed. The middle curve is the annually repeating component (with arbitrary mean), and the lower curve is the remainder after subtracting the polynomial and annually repeating components from the complete time series (again, with arbitrary mean).

term drift and annually repeating part are extracted by simultaneous least squares fitting of a fifth-order polynomial and 12 monthly values with linear interpolation between them (this form is chosen to match that of the wind forcing). Since FRAM is a rigid-lid model, and the streamfunction is set to the same constant on South America, Africa, and Australia, the transports south of these three continents are equal at all times.

The rigid-lid formulation also avoids the use of pressure in the model calculations, although pressure gradients can be inferred (at model velocity points) from the model dynamics. Pressures are then calculated at tracer grid points by integration of the gradients. (The finite difference procedure permits the pressure difference between diagonally opposed corners of the velocity grid box to be calculated from the gradient at the velocity point. The pressure gradient was integrated in an ad hoc manner until the whole model domain had been covered.) This procedure is necessarily approximate since the pressure gradients do not have exactly zero curl due to imperfect convergence of the streamfunction calculation, so there is no unambiguous pressure field. Even so, the pressures calculated are consistent to within 10 Pa (0.1 mb, or approximately 1 mm of water), as was shown by comparing pressures on either side of the periodic boundary. Two constants have to be chosen in this procedure: the spatial average pressures on the two grids produced by integration in diagonal steps. The difference in constants was chosen to minimize ''checkerboarding,'' and then the sum was chosen to give zero area average. Since this procedure was followed using surface pressures, mass is not precisely conserved when density changes occur. However, the density forcing is by relaxation to annual mean Levitus values in the surface layer and has no significant seasonal cycle.

Figure 3 immediately tells us several things about the transport fluctuations in FRAM. Since the winds are annually repeating, neither the long-term trend nor the shorter period fluctuations can be attributed to the wind forcing. The long-term trend is a climate drift of the model and may be attributable to the lack of Antarctic Bottom Water formation (Killworth and Nanneh 1994) or other transient thermohaline effects, demonstrating how the thermohaline circulation can affect transport on interannual timescales. The other nonrepeating component must be intrinsic (i.e., unforced) fluctuations due to nonlinear activity within the current since there is no forcing on timescales shorter than a month. It is noteworthy that, although smaller in magnitude than the annually repeating component, these fluctuations are not negligible, even in FRAM, which has a less energetic eddy field than the real ocean (Stevens and Killworth 1992).

Woodworth et al. (1996) presented correlations of subsurface and bottom pressure (with a linear climate drift removed) with transport, from FRAM. The resulting plots (particularly for bottom pressure, for which the eddy field is less intrusive) clearly show the influence of the f/H contours shown in Fig. 2 and demonstrate that it is pressure to the south of the ACC that is (negatively) correlated with transport. Some statistically significant positive correlations are seen to the north, but these are unlikely to be realistic since all occur on f/H contours directly connected to the northern open boundary, where a flat-bottom Sverdrup balance is applied (Stevens 1991). The significant positive correlations on the Patagonian shelf, north of Drake Passage, are worth noting though, especially as similar correlations are not seen at the northern ends of the other choke points south of Africa and Australia. These plots are not reproduced here, but see the later section using POCM data for similar plots. The FRAM domain only extends to 24°S, so the ''rest of the World Ocean'' is rather smaller in FRAM than in reality; but it is still pressure to the south that reflects transport.

In an attempt to define the patch of the current that is responsible for transport fluctuations, while minimizing the effect of eddies, a set of streamfunction fields was spatially smoothed using a 21×21 gridpoint running mean filter. For each grid point of the resulting 95 smoothed streamfunction fields (streamfunction at 10-day intervals), a simultaneous fit was performed to the polynomial and annually repeating transport time series of Fig. 3. The resulting annually repeating fit is shown in Fig. 4. The streamfunction on northern land masses is zero in FRAM, so the fit is close to zero here and close to 1 around Antarctica. If the transport current follows a preferred path, it will show up as the region of highest gradient. Except in the eastern Indian Ocean sector, where the fit is large but correlations are poor, the current tends to follow the f/H contours highlighted in Fig. 2 (although the response in the Weddell Sea is odd, but still related to f/H contours).

A second way to look at the path of the current in FRAM is in terms of the fit between bottom pressure and transport. Since the correlation is very good close to Antarctica, the fit can be used to define an effective f/H or H/f, as defined in (12). This was calculated by choosing the first minimum (i.e., most negative value)

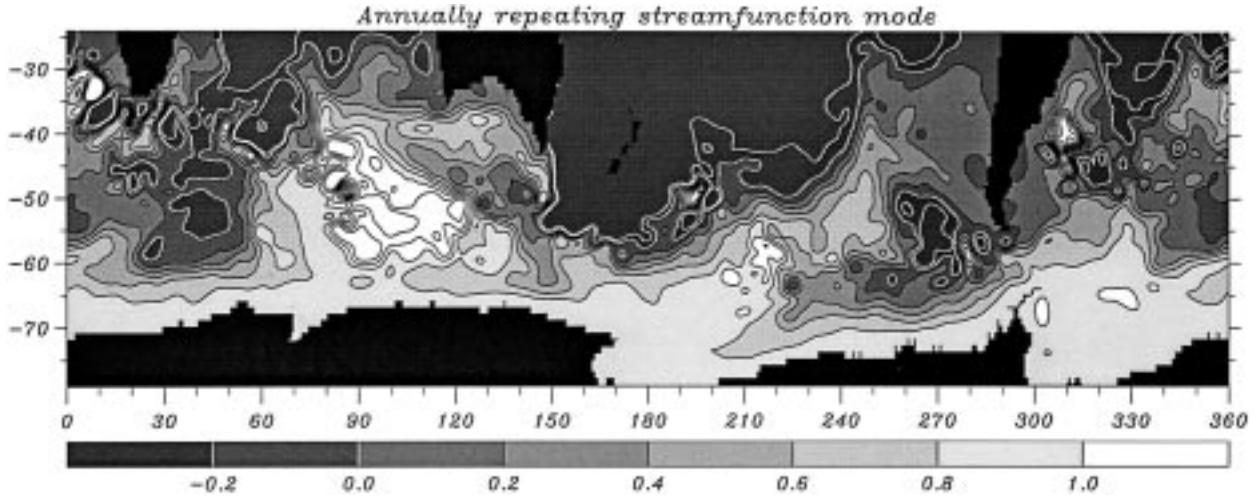

FIG. 4. The fit of spatially smoothed streamfunction (from 95 fields at 10-day intervals) on the annually repeating transport time series. Contours are at intervals of 0.2, from −0.4 to +1.4; positive contours are black.

of the fit of bottom pressure on transport as one travels northward from Antarctica (the first minimum was chosen to avoid strong influence from boundary friction). The result is plotted in Fig. 5. Again, the path of the current in Fig. 4 closely matches the contour, although there are places where the current jumps from one branch of the contour to another. The clearest example is in Drake Passage, where no contour exists for some longitudes. This means that there is no value of H/f large enough in Drake Passage for the transport to be

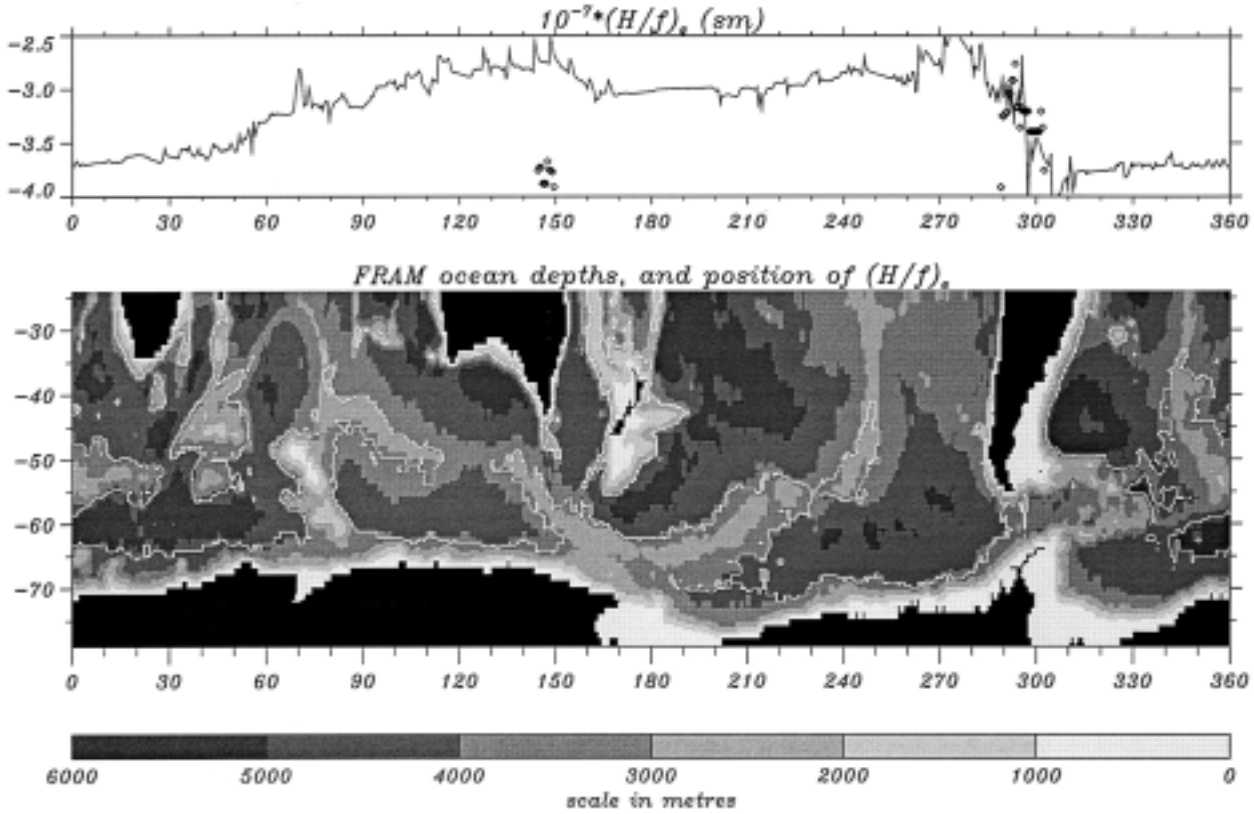

FIG. 5. The effective value of H/f, defined by (11), and calculated at each longitude from the linear fit of bottom pressure near Antarctica on volume transport. (top) Also shows the largest (negative) value of H/f at each longitude (diamonds); (bottom) the position of this H/f contour, superimposed on the model topography.

produced entirely by geostrophic barotropic fluctuations at the south: the pressure change is too small to account for the transport change for a current with any distribution of latitudes, at these longitudes. The upper panel of Fig. 5 has diamonds marked on it, representing the most negative value of f/H found at each longitude in FRAM. Where these lie above the line, the relationship between bottom pressure and transport cannot be explained by barotropic geostrophic currents. This only happens in Drake Passage, and there only by a small margin, or over very short length scales, which can easily be accounted for by nonlinear processes, mesoscale baroclinic fluctuations, and statistical uncertainties in the linear fit of pressure on transport. Nonetheless, it seems likely that this is related to the positive correlations seen to the north of Drake Passage, perhaps reflecting a part of the transport through the passage that occurs in the Sverdrup mode. The value of H/f shown in the upper panel lies in the lightly shaded region of Fig. 2, except east of Drake Passage to 60°E where it moves to the deeper (unshaded) region. Thus, this response seems more closely related to the almost free mode than to the free mode.

The model can also be used to test the assumptions of depth independence and geostrophy. While the above results on the importance of f/H contours are strongly indicative of a large-scale barotropic mode, it is not clear that the barotropic signal will be the dominant signal at any one place. To test this, transports were calculated from the FRAM data at five sections: south of South Africa, western Australia, central Australia, east Australia, and in Drake Passage. The results from south of South Africa are not shown, as the baroclinic transports here are enormous due to the proximity of the high-variability Agulhas retroflection to the coast. Transports from the other sections are shown in Fig. 6.

It is clear from this figure that the transport fluctuations are mostly geostrophic, although some significant ageostrophic fluctuations occur. What is more striking is that the variability at each section is not barotropic. (Recall that the argument in favor of a barotropic response depends on an assumption of a suitably large length scale. We might expect baroclinic effects to be important at a single meridional section with an effective zonal length scale of one grid point.) Depending on the reference depth, the baroclinic transport fluctuations can be comparable to, and sometimes larger than, the total. For the Drake Passage and western Australia sections, the baroclinic transport fluctuations relative to 2391.5 m are quite small, so this depth may serve as a good reference depth for the barotropic flow. This seems to contradict the finding of Whitworth and Peterson (1985) that 500 m provides a good reference level, but they were only concerned with transport above 2500 m. A shallower reference level must be expected for this component of the transport variability, but the FRAM results suggest that flow fluctuations deeper than 2500 m form an important component of the total transport variability, making a deeper reference level appropriate for estimates of variability in the total transport. However, it would probably be pushing the FRAM data too far to recommend a reference depth in a place like Drake Passage where the approximate topography produces large distortions in the modeled mean flow (Grose et al. 1995).

The vertical distribution and behavior in time of the baroclinic transport fluctuations differ quite markedly, even between the three Australian sections, demonstrating that there is no zonally coherent mode in the baroclinic transport. It seems that the total transport across a section is made up of both barotropic and baroclinic components but, whereas the total flow must exhibit zonal coherence, the form of the baroclinic flow is coherent only over short distances. At any one place then, it is impossible to separate the large-scale barotropic mode that is guided by f/H contours from the smaller-scale baroclinic fluctuations. The exception to this is to the south of the ACC, where stratification becomes weak enough for the baroclinic fluctuations to be small. In addition, the waveguiding effect of f/H contours ensures that this barotropic signal is representative of a broad range of longitudes. Here, it seems, is a second reason for bottom pressure to the south of the ACC to be a much more reliable indicator of transport fluctuations than pressures farther north.

This problem of local baroclinic activity masking the large-scale signal has been noted several times before. Peterson (1988a) notes a peak at about the 1.5-month period in the bottom pressure spectrum from the northern ISOS records, which he attributes to mesoscale eddy activity. Johnson (1990) attempts to explain the lack of a clear relationship between these northern Drake Passage measurements and zonal wind stress in terms of coastally trapped waves propagating southward along the western coast of South America. Meredith et al. (1996) conclude that the ND1 record is unsuitable for monitoring transport variability because it is dominated by movements of the Sub-Antarctic Front, and also note that the Myrtle record (another BPR system situated about 100 km north of the SD2 position) is dominated by local processes for periods longer than about 4 days. This conclusion is consistent with the relatively poor agreement between altimeter-derived subsurface pressures and bottom pressure at the Myrtle site (Woodworth et al. 1996).

Finally, the FRAM data can be used to look at the relationship between transport fluctuations and winds. Since the winds repeat exactly from year to year, we have the advantage that we can filter out many of the nonwind effects by considering the annually repeating transport time series from Fig. 3. No useful spectral information can be extracted since we are now comparing 12 monthly values of transport with 12 numbers derived from the monthly wind fields, so a correlation coefficient is the best that can be done.

Five time series were calculated from the wind fields:

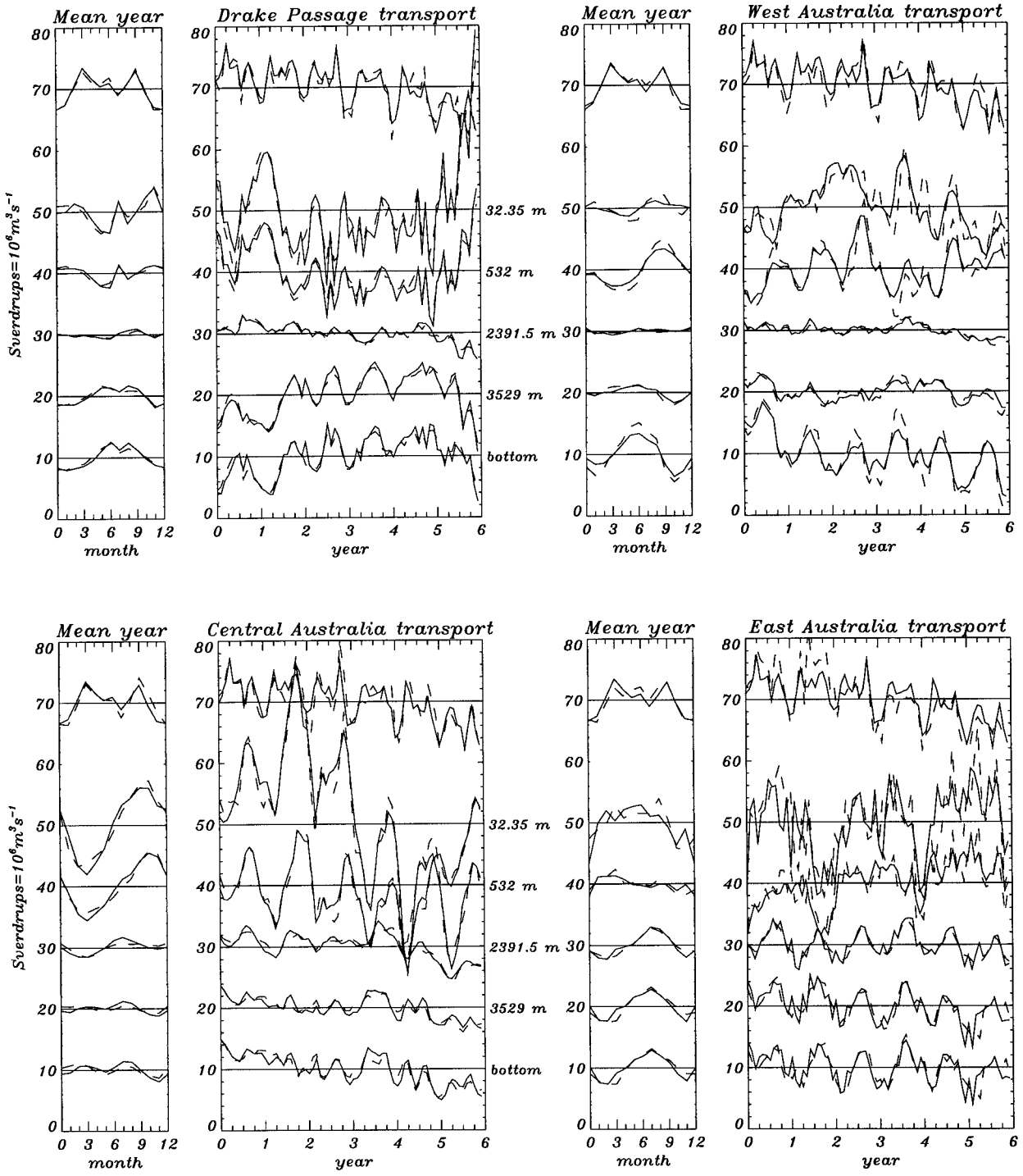

FIG. 6. Time series of (solid lines) total transport and (dashed lines) geostrophic transport through meridional sections of FRAM at Drake Passage (289°E), western Australia (119°E), central Australia (131.5°E), and east Australia (144°E). In each panel, the top line shows the complete transport, and lower lines show baroclinic transport relative to reference depths of 32.35, 532, 2391.5, 3529 m, and the bottom. Mean values are arbitrary. Where the reference depth is deeper than the ocean, the bottom is taken as reference depth.

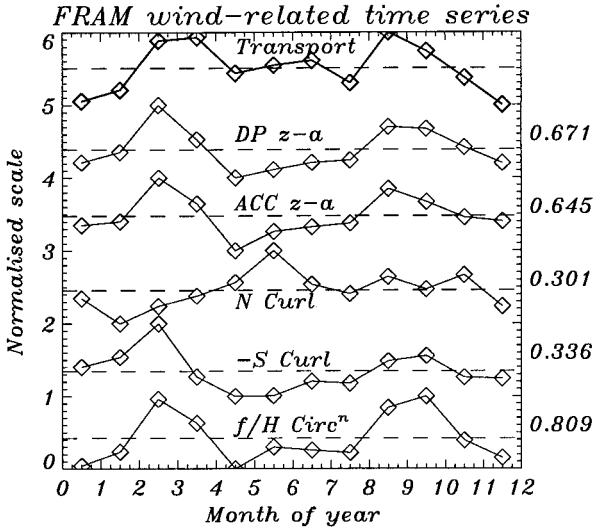

FIG. 7. Annual time series of transport and five integrated measures of wind stress (defined in the text), from FRAM. Correlation coefficients between each wind stress time series and the transport are shown to the right. A coefficient of 0.576 is significant at the 95% level.

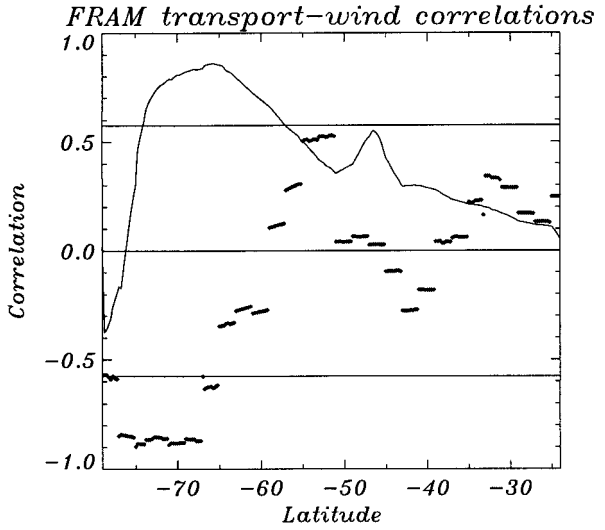

FIG. 8. Correlation coefficients between annually repeating transport from FRAM and (line) zonal average eastward wind stress τ; (diamonds) zonal integral of curl (τ/f). The value of correlation significant at the 95% level is also marked.

zonal average of eastward wind stress through the Drake Passage latitudes (DP z-a); zonal average of eastward wind stress over the ACC, defined as the area between the 0 and 180 Sv streamlines that pass through Drake Passage (ACC z-a); zonal integral of the wind stress curl at the northernmost latitude of Drake Passage (N curl); zonal integral of the wind stress curl at the southernmost latitude of Drake Passage (S Curl); and integral of tangential wind stress along the northernmost f/H contour ($f/H = -4 \times 10^{-8}$ s^{-1} m^{-1}, $H/f = -2.5 \times 10^{7}$ s m) to pass right around Antarctica (f/H Circ^n). Figure 7 shows these time series, together with the transport time series, with correlation coefficients between the winds and transport. The 95% significance level requires a correlation coefficient of 0.576. Neither of the wind curl time series is significant at this level, although the difference (N Curl − S Curl) gives a correlation coefficient of 0.596. The difference time series is, of necessity, strongly correlated with the DP z-a time series. The strongest correlation is clearly with winds averaged along the f/H contour, although other measures of the wind field to the south of Drake Passage give similar correlations, as illustrated in Fig. 8. This figure shows the correlation between transport and zonally averaged eastward wind stress (line), and zonally integrated wind stress curl (diamonds), at each latitude in FRAM (with the 95% significance value superimposed). The highest correlation for wind is at about 65°S, approximately the southernmost latitude of Drake Passage, and even higher correlations are found for wind stress curl south of this latitude. Once again, the FRAM data favor a southern mode for the transport variability, consistent with the idea of a barotropic current following f/H contours (either a free mode or an almost free mode). The zonal averages were only calculated for wind stresses over the sea. South of about 67°S, a significant fraction of a latitude circle is occupied by land, so values this far south are only representative of a limited longitude range. The maximum correlation at 65°S for zonal average winds is then what might be expected, although the high correlations for curl farther south are curious.

5. Bottom pressure measurements

As described in the introduction, instruments have been deployed to the north and south of Drake Passage, at various positions, since 1989. Figure 9 summarizes the duration and depth of each deployment at the positions marked on Fig. 1. The end of one time series and the start of the next are typically separated by a gap (or sometimes an overlap) of one or two days. In addition, each BPR record suffers from a long period drift. An attempt has been made to remove this drift by fitting a low-order polynomial to the records and examining

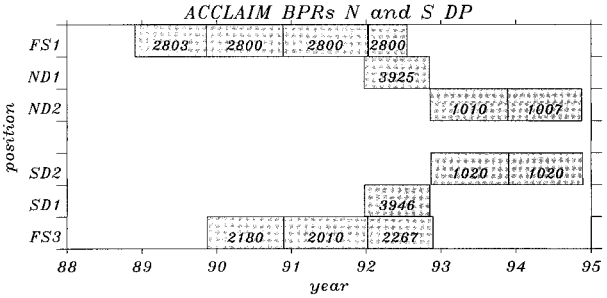

FIG. 9. Schematic showing the duration and depth of deployment (m) of the BPRs at positions shown in Fig. 1.

the residuals. There were three pressure sensors on each BPR, and the order of the polynomial fit was the minimum that allowed the long period behavior of the residuals to match. This was usually a linear fit, but in some cases a quadratic fit was necessary. It is hard to tell how successful this has been, so the BPR records must be regarded as suspect for annual and longer periods. A one cycle per day tide-killing filter has been applied, and the BPR datasets resampled at daily intervals.

For comparison with the BPR records, wind stresses calculated from the European Centre for Medium-Range Weather Forecasts (ECMWF) meteorological analyses were used. Of the time series of Southern Ocean winds available over the whole time considered here, the ECMWF analyses were described by Trenberth (1992) as being the most reliable. The particular dataset used is the ECMWF Tropical Ocean–Global Atmosphere analysis, which runs from 1985 to the end of 1994. Full details of the assimilation schemes and physical parameterizations used in this analysis can be found in ECMWF (1991, 1992).

Wind stresses were computed from the 10-m winds in this analysis, and supplied for 12-h intervals on a 2.5° grid by the U.S. National Center for Atmospheric Research. A standard quadratic bulk formula was used, with a neutral drag coefficient following those of Large and Pond (1982), Dittmer (1977), and Schacher et al. (1981). For comparison with the BPR data, daily values were computed from the 12-h values as $0.25 \times (\tau_{-12} + 2\tau_0 + \tau_{+12})$, where τ_0 is the wind stress at midday, and the other values are at the previous and following midnight.

Six time series were calculated from the wind stresses: three zonal averages and three zonally integrated wind-stress curls. The three zonal averages are integrated over the ranges 40°–65°S [similar to the range used by Peterson (1988a) and referred to here as the ACC region], 55°–62.5°S (approximately the Drake Passage latitudes, referred to here as DP), and 60°–65°S (south of Drake passage, referred to here as South). The curls are integrated over ranges 40°–45°S [similar to the northern curl region of Peterson (1988a) and referred to here as Curl far N], 52.5°–57.5°S (at the northern end of Drake Passage; Curl N), and 60°–65°S [the southern end of Drake Passage, similar to the southern curl region of Peterson (1988a); Curl S].

In order to see if any useful long-period information is contained in the BPR records, concatenated time series were constructed by end point matching. For this procedure, a 60-day low-pass filter was applied to the individual records, and a linear extrapolation made to the central times between BPR records. A datum shift was then applied to each record to match up the extrapolated values. The four FS1 time series were concatenated in this way, as were the two ND2 time series. In view of the similarity observed between records at different southern sites (Woodworth et al. 1996; Meredith et al. 1996), the five FS3 and SD2 time series were concatenated into a single time series.

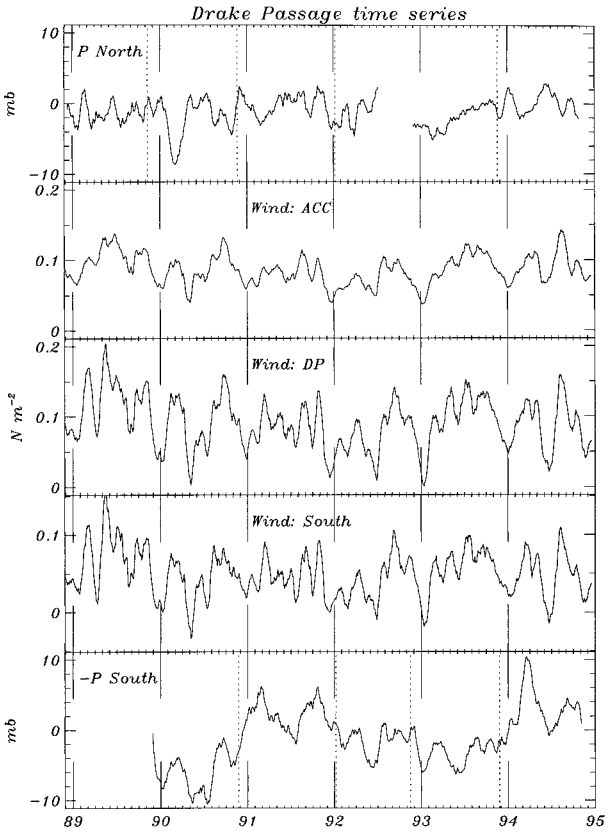

FIG. 10. Time series of bottom pressure and zonally averaged ECMWF-derived wind stresses. Dashed lines mark where the pressure time series have been joined by end point matching. Here P north consists of the records from FS1 and ND2, P south is shown inverted and consists of records from FS3 and SD2. The wind time series are defined in the text. Each time series has been smoothed with a 29-day running mean.

The concatenated BPR time series (southern pressure is shown inverted), and the three zonally averaged wind stress time series, are shown in Fig. 10, after application of a 29-day running average smoother for display purposes only (this effectively removes the fortnightly and monthly tides). Dashed lines show where end point matching has been used to join up the time series. Visual inspection is enough to see that the three wind stress time series are strongly correlated, highlighting the difficulty in establishing a forcing mechanism for any correlations with bottom pressure. Correlations with bottom pressures are much less obvious, unless the time series are broken at the dashed lines, when a correlation can be discerned between southern pressures and winds. No consistent correlation is apparent between winds and northern pressures. In order to quantify the agreements and examine their frequency dependence, cross-spectra were calculated using both concatenated time series, and all of the individual (1 yr) time series (including ND1 and SD1). For the northern pressures, the only squared

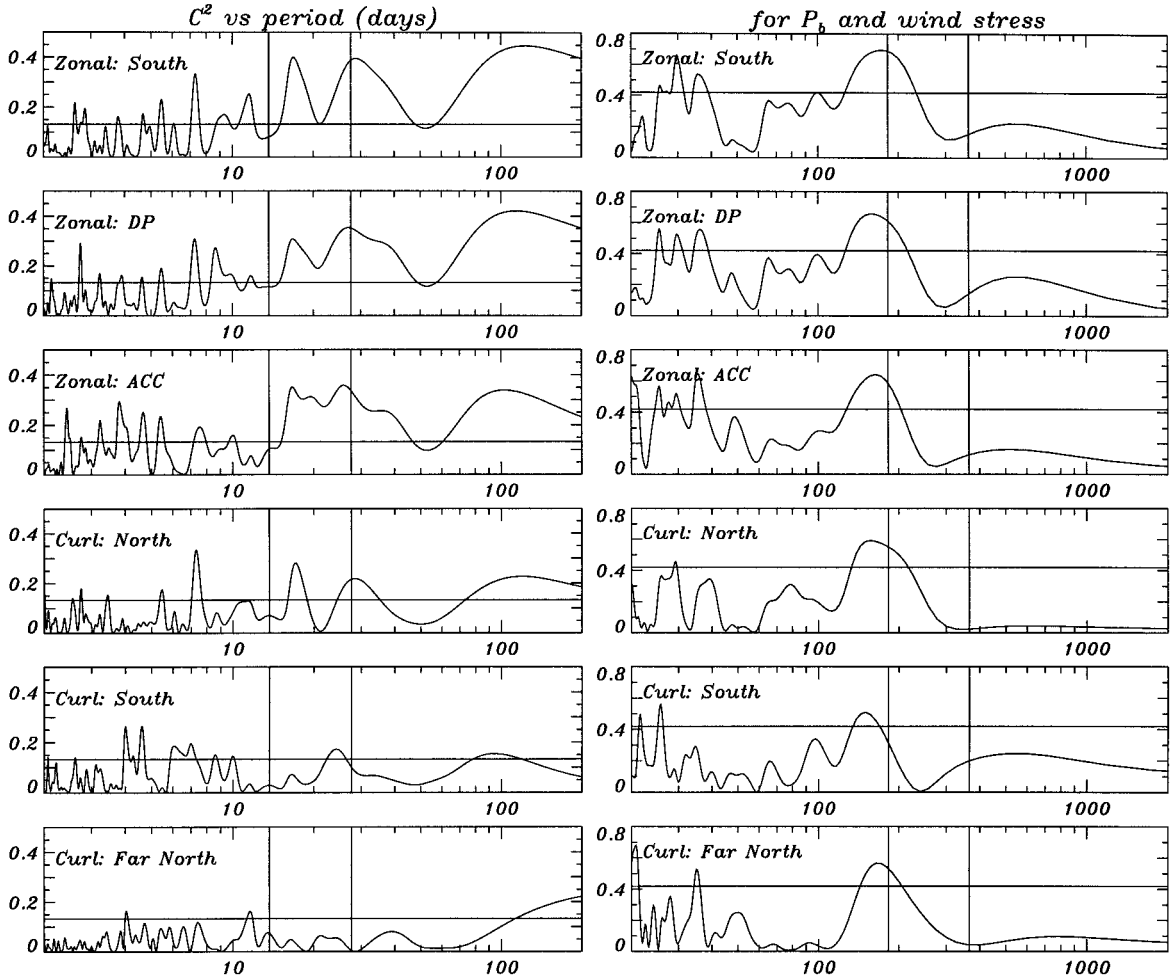

FIG. 11. Squared coherences from cross-spectra between southern bottom pressure and six integrated wind time series. The 95% significance value is marked in each panel, as are the fortnightly and monthly tidal periods in the left-hand panels, and semiannual and annual periods on the right. Values on the left are calculated treating each BPR deployment separately, using a 90-day window half-width; those on the right are calculated from the concatenated pressure time series using a 360-day window half-width.

coherences that were significant at the 95% level were for wind stress–pressure correlations at periods of about 10 and 20 days (in light of the theory discussed above, the frequency range of interest is periods longer than 10 days; some squared coherences are significant at shorter periods). Pressure to the north is not significantly coherent with pressure to the south for periods longer than 10 days. In view of the poor coherences and the theoretical arguments favoring bottom pressure to the south as a measure of transport, the northern pressures will not be discussed further.

Figure 11 shows squared coherences for cross-spectra between southern pressure and each of the six wind fields. The cross-spectra were calculated by computing auto- and cross-covariances, multiplying the covariances by a Tukey [$0.5 \times (1 + \cos)$] window and Fourier transforming. For the left-hand plot, the covariances were calculated only using pairs of values from the same BPR deployment, and the window half-width was 90 days. The 95% significance value is calculated assuming an effective time series length corresponding to the smallest number of pairs used to calculate a covariance. This value, and the monthly and fortnightly tidal periods, are marked on the figure. The right-hand panel shows values calculated using the concatenated time series, with a window half-width of 360 days. The 95% significance value is again marked, together with the semiannual and annual periods. Significant coherences are found at all periods between about 15 and 220 days, with the exception of a window around 50 days (this may be related to the Indonesian Throughflow; see later). At almost all of these periods, the highest coherence is with zonally averaged wind stress south of Drake Passage, although all the zonal averages give high coherences. Coherences with wind stress curl are generally much lower. The curious exception to this pattern is at periods close to 20 days, where the zonal averages including winds from farther north do better. As a visual

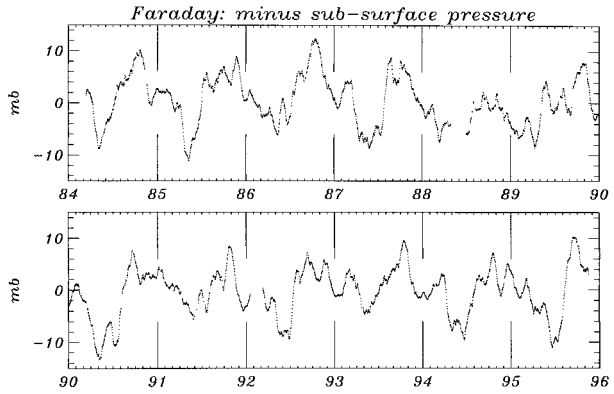

FIG. 12. The negative of the subsurface pressure record from Faraday, smoothed with a 29-day running mean.

inspection of the time series showed, coherences at annual and longer periods are poor, suggesting either that the dynamics on these timescales are dominated by factors other than wind stress or that end point matching of the time series fails to capture the long-period pressure variability. Both of these scenarios are plausible.

If the end-point matching is doing a poor job of capturing the long-period variability, then a long, continuous pressure record is needed for annual periods and longer. Such a record is available from the tide gauge maintained by POL at the British Antarctic Survey (BAS) base, Faraday (now owned by the Ukraine and renamed Vernadsky). Peterson (1988b) noted that the subsurface pressure at Faraday, calculated by converting sea level to pressure units and adding the atmospheric pressure, was strongly coherent with the ISOS southern BPR record for periods of about 6 to 600 days, although a phase shift of about 60° occurred at the annual period (coherence was barely significant at the 95% level for this period, so the phase shift will have a large standard error). A similarly calculated time series is shown in Fig. 12, using daily atmospheric pressures from the BAS meteorological database, and with a 29-day running mean filter applied.

Figure 13 shows cross-spectra between pairs of the three time series, concatenated bottom pressure record from southern BPRs, Faraday sea surface pressure (SSP), and zonally averaged winds (south), calculated with a window half-width of 360 days. A broad range of high coherence is clear between bottom pressure and Faraday SSP, although this does not extend to the annual period as Peterson (1988b) found. Phase is close to zero over all of this coherent range. Faraday SSP shows a now-familiar pattern of coherence with the winds, with a dip around a 50-day period, and a high semiannual coherence. Compared with the BPRs, the Faraday record shows higher coherence with the winds at an annual period and close to 20 days. Phase lags are near zero for periods between about 15 and 200 days with a phase lag of about 65° at the annual period (winds lead transport). The long-period coherences with winds are higher for Faraday than for the BPRs, indicating that the Faraday record may be the better monitor of circumpolar transport at annual periods and longer, but the Faraday record is complicated by its coastal situation. Higher coherence with winds may be at least partly attributable to local coastal processes, so it is still not clear that transport fluctuations are strongly influenced by the wind at the annual period, although the significant coherence is suggestive of this. Formation and melting of ice will certainly produce a steric signal at the annual period, which may predominate over the wind forcing.

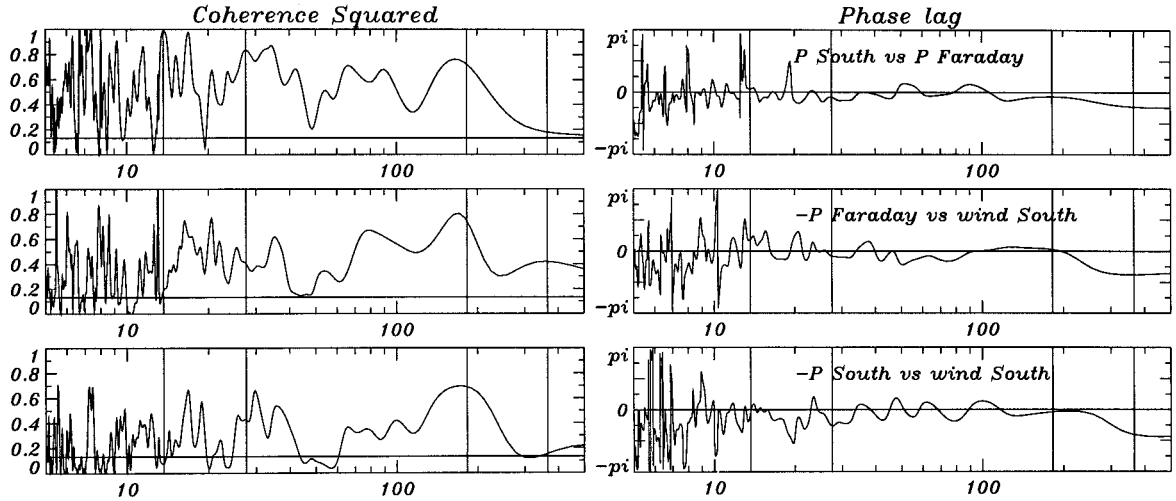

FIG. 13. Squared coherences and phase for cross-spectra between (top) the concatenated southern BPR record and Faraday subsurface pressure; (center) Faraday subsurface pressure (inverted) and zonally averaged southern wind stress; and (bottom) the concatenated southern BPR record (inverted) and zonally averaged southern wind stress. Spectra are calculated using a 360-day window half-width, and the 95% significance values are shown, together with semiannual and annual periods and monthly and fortnightly tidal periods. Periods are marked in days, and positive phase means that the second named time series lags the first.

6. Model results with realistic forcing

So far, a model (FRAM) with simplified forcing has been used, along with theoretical arguments, to determine the nature of the Southern Ocean's response to winds on the barotropic timescale. The simplified forcing (climatological monthly winds) is in some ways an advantage for identifying the mechanism behind the response, but precludes direct comparison between model and data as well as severely limiting the investigation of the frequency dependence of the dynamics. For this, we need a model, preferably eddy permitting, that is forced with winds as close to the real winds as possible.

Such a model is the ¼° (average) Parallel Ocean Climate Model (POCM) described by Stammer et al. (1996) and Semtner and Chervin (1992). This model is basically similar to a global (apart from the Arctic) version of FRAM except that it uses a free surface formulation that removes the need to smooth the topography beyond the grid resolution, although the vertical resolution is less than FRAM with only 20 levels. The resolution of this model increases toward the poles on a Mercator grid, giving square grid cells 0.4° of longitude wide, between the equator and latitude 75° (equivalent to about 28.5 km at 50°S, 15.2 km at 70°S).

The version of the model used here is POCM_4B for the period 1988 to 1996. This version was forced by 3-day averages of wind stresses derived from ECMWF 10-m winds (Stammer et al. 1996) starting from 1987. Results from 1987 are not considered here as the transport dropped throughout this year from an initial value near 192 Sv to a mean value of 166 Sv, as a response to the change from an overestimated climatalogical wind stress applied in a previous version of the model.

The 3-day sampling of the model field produces an aliasing of inertial oscillations to different periods between 6 days and infinity at different latitudes (Jayne and Tokmakian 1997). These are clearly visible in time series of velocity and are unlikely to be realistic when forced by 3-day winds; however, the variation of an aliased period with latitude has a mitigating effect when calculating transports, and inertial oscillations do not appear to be a large problem here.

Transports were calculated as integrals of the zonal velocities across the five meridional sections used in FRAM. These now differ from section to section because the model allows an Indonesian Throughflow from the Pacific to the Indian Ocean, and the free surface allows a small divergence of the depth-integrated flow. The sections south of Africa and South America show standard deviations of 6.25 and 6.15 Sv, respectively, and the difference time series has a standard deviation of 1.66 Sv, part of which may be aliased inertial oscillations (the discrepancy is greatest at periods shorter than 15 days, consistent with aliassed inertial oscillations south of about 60°S). In contrast, the difference between transport through Drake Passage and south of Australia has a standard deviation of about 5.2 Sv, demonstrating the importance of the Indonesian Throughflow here. The time series chosen for comparison with winds and measurements is the transport through Drake Passage, sampled every 3 days. Practically identical results are found using the African section.

With realistic forcing, it must be hoped that the model will produce realistic transports. If this is the case and Faraday subsurface pressure is a good monitor of transport, then the two time series should be highly correlated. Figure 14a shows the cross-spectrum of these time series for the period 1988 to 1995. Coherence is significant at many frequencies between about 10 days and the semiannual period, with particularly high values between about 80 days and the semiannual period (the range that FRAM is most sensitive to is about 60 days to annual). Phases are also close to zero over the regions of high coherence. The low coherence for periods longer than semiannual suggest that either processes other than transport fluctuations dominate the Faraday pressure signal at the annual period or the model transports at annual period are particularly poor.

Figure 14b shows cross-spectra between zonal averages of model eastward wind stress at six latitudes and model transport. For the 10-day to semiannual period band, coherences increase southward from 45°S, peaking at around 60°–65°S. For periods longer than semiannual, the winds as far north as 50°S seem to be most important, suggesting that a different mode dominates at the annual period. The dip in coherence seen in the measurements at 50 days is also present in the model results. It is interesting to note that the coherence between transports south of Africa and Australia is smallest (and not quite significant at the 95% level) at about 47 days, suggesting that this feature might be related to the Indonesian throughflow and thus to the dynamics of tropical 40–60 day oscillations.

For a pure free mode response to winds, transport should respond with a phase lag of $\pi/2$. For a forced (topographic Sverdrup) response the phase lag would be $\pi/2$ for periods much shorter than the relevant topographic Rossby wave mode and would represent a small lag for longer periods. Friction would give a similar picture to the forced response, with the relevant time being the frictional spindown time. The phases in Figs. 13 and 14 show that a lag of $\pi/2$ is not attained for any period longer than about 10 days, so the pure free mode response can only be relevant for very short periods. As suggested at the end of the ''dynamics'' section, an almost-free mode, for which f/H contours are not quite closed, is probably important. This mode will be particularly sensitive to winds in the regions where it is necessary for the current to cross f/H contours and will react to these winds with a ''forced'' rather than free response.

The POCM model transport fluctuations, like those in FRAM, are most strongly related to sea level fluctuations south of Drake Passage, as shown by the correlation coefficient between transports through Drake

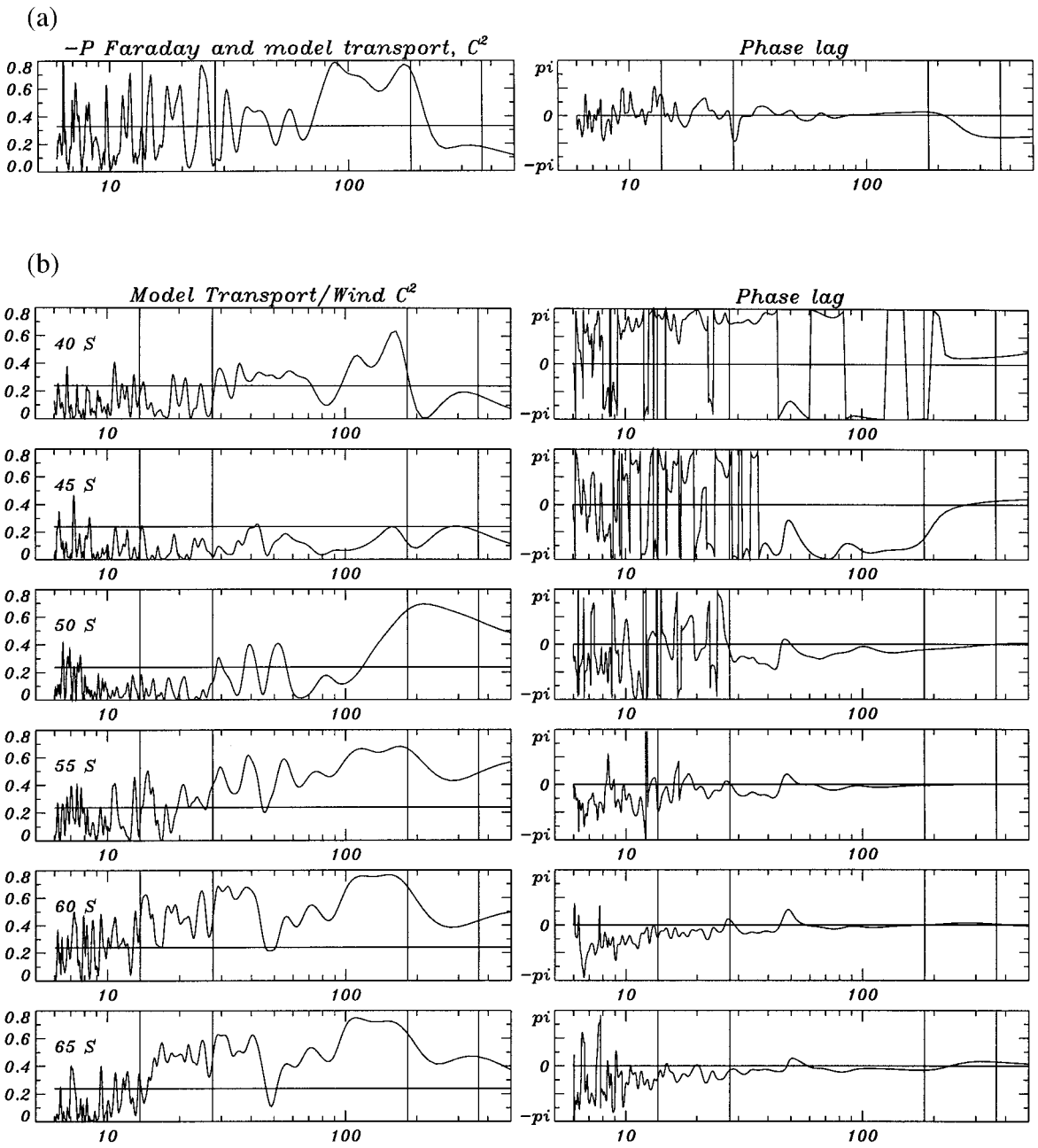

FIG. 14. Cross-spectra as in Fig. 13 for (a) minus Faraday subsurface pressure and POCM-4B model transport through Drake Passage and (b) model transport and zonally averaged model wind stresses at six latitudes.

Passage or south of Australia and 9.9-day averaged sea surface heights (Fig. 15). Since the transports through Drake Passage and south of Australia differ significantly in this model, the correlation with each of these time series is given. In both cases the southern mode is dominant with (negative) correlations greater than 0.6 occuring at almost all longitudes, peaking at more than 0.75. The northern correlations differ dramatically between the two cases. For the transport south of Australia, positive correlations on the Australian shelf are typically 0.4 to 0.6 (with a peak value of 0.621), but only very small correlations occur to the north of Drake Passage. Conversely for Drake Passage transport, the correlation with sea surface height close to Australia is very small, but correlations of 0.4 to 0.45 occur near the southern tip of South America, peaking at 0.464 to the northeast of Drake Passage. Interestingly, similarly high correlations occur off the coast of Alaska peaking at 0.461, and in regions of the northeast and southeast Pacific. Lagged correlations trace the origin of this signal to the

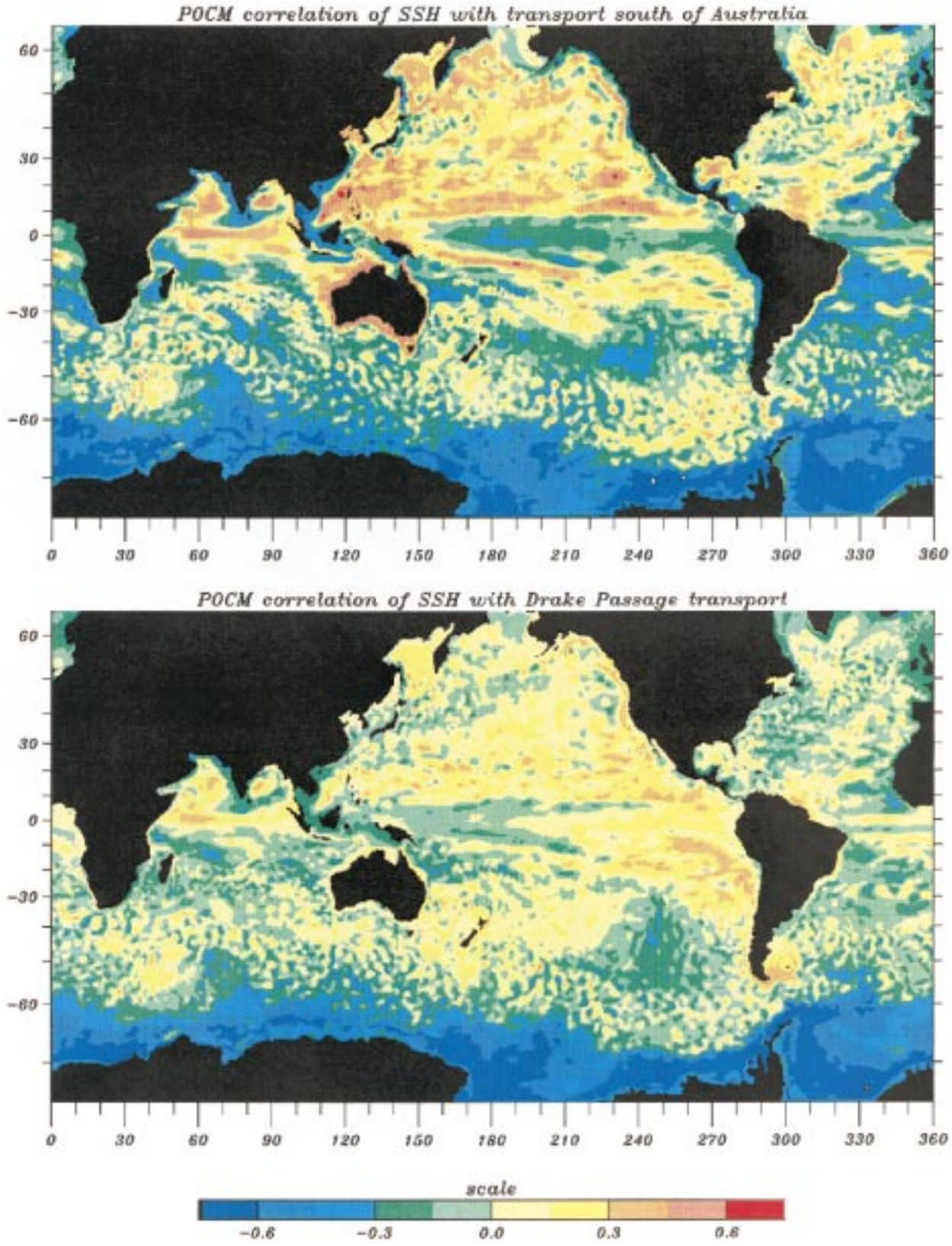

FIG. 15. Correlation coefficients between 9.9-day averaged sea surface heights and transport through (top) the region south of Australia and (bottom) Drake Passage, from the POCM.

eastern equatorial Pacific and produce patterns consistent with the propagation of coastal Kelvin waves to both north and south, radiating Rossby waves into the Pacific before arriving at Drake Passage and Alaska. The patch of moderately high correlations centered on 50°S, 250°E, is negative, consistent with Fig. 4 which shows the current passing to the north of this region. Another interesting point is the very low correlations near the South African coast. This is not due to the small difference between transports through Drake Passage and south of Africa since the equivalent correlation plot calculated using transport south of Africa (not shown) is practically indistinguishable from that using Drake Passage transport.

Quantitative interpretation of the significance of these correlations should be treated with extreme caution, as the time series involved may have significant annual and semiannual components. To give some quantitative guidance however, assuming each of the 148 9.9-day averages to be independent, a correlation coefficient of 0.16 would be significant at the 95% level. Assuming every third value to be independent (probably more realistic), this increases to 0.27. Correlations of transports with pure semiannual and annual signals have the following maximum possible values: Drake Passage transport with semiannual, 0.224; with annual, 0.356. Transport south of Australia with semiannual, 0.176; with annual, 0.683. Thus, the relatively high correlations between transport south of Australia and sea levels in the North Pacific and Indian Oceans are probably simply due to a favorable phase of the annual signal.

Thus, the POCM data seem to confirm that the positive correlations north of Drake Passage are real, but they are not representative of the flow over a broad range of longitudes in the way that southern pressure is. In particular, northern pressure in Drake Passage is very weakly related to flow south of Australia, and vice versa. The relationship with the dynamics of the equatorial Pacific suggests that baroclinic effects are likely to be important in interpreting the northern pressure signal, and is consistent with the failure to find a clear relationship between northern pressure and winds over the Southern Ocean.

7. Discussion

Theoretical arguments have suggested that transport fluctuations through Drake Passage may be dominated by a barotropic mode that follows f/H contours around much of Antarctica. It has been shown using FRAM that, while the barotropic mode might be locally swamped by baroclinic variability, it forms a good description of the larger-scale variations in the model. Both theoretical arguments and model results support the idea that it is pressure to the south of Drake Passage that is the best monitor of transport fluctuations, although northern pressures may be related to local transport in a more complicated way. This is in line with past observations of correlations between wind stress and southern pressure, from the ISOS experiment (Wearn and Baker 1980; Peterson 1988a).

Given the strong correlations between different measures of the wind forcing in the Southern Ocean, a convincing demonstration that this model applies to the real ocean is difficult to achieve using only observational data. However, cross-spectra between bottom pressure and winds show slightly better coherences with winds to the south of Drake Passage than with other measures of wind stress, and the POCM model results show that the measured bottom pressure fluctuations south of Drake Passage are highly correlated with model transport. A number of features suggest that it is not the inviscid free mode response that dominates, but either a viscously damped free mode or the almost free mode that requires wind forcing for the current to cross f/H contours in certain locations. The small phase lag between winds and both pressure and POCM transport is consistent with either of these interpretations.

There is some evidence for the importance of the almost free mode in FRAM: although the current seen in FRAM follows f/H contours most of the time, there are places where it has to skip across a few contours. If correlation coefficients are calculated between FRAM transport and eastward wind stress at each grid point, several ''hot spots'' of high correlation appear (D. Stevens 1996, personal communication). Two of these hot spots are between the southern tip of South America and the Falkland Islands and over the Scotia island arc, regions where the current appears to skip over f/H contours. The third is at about 40°S, 230°E, at a sensitive point where f/H contours can either return along the Pacific Antarctic Rise or can cut across the top of the South Pacific basin. It therefore seems reasonable that the almost-free mode should be particularly sensitive to winds in these regions. The fact that these hot spots occur east and west of South America may also offer an explanation for the positive transport–pressure correlation seen in FRAM over the Patagonian shelf, suggesting that the Sverdrup mode also plays a role in the region of Drake Passage where the range of f/H contours is narrowest. In the POCM, the northern correlations still occur but are further complicated by the fact that the associated sea surface height anomalies seem to have their origin in the equatorial Pacific, propagating to the south (and north) as coastal Kelvin waves.

An interesting feature in both the pressure measurements and the POCM transports is a relatively poor coherence with southern winds at a period of about 50 days. Suggestively, this is the same period at which the POCM results show that the Indonesian Throughflow is most influential in decoupling transports south of Australia from the other choke point transports, which may imply a link with the 40–60 day tropical oscillations, although further investigations are needed to confirm this link.

The idea of a more southerly mode for the transport

fluctuations should be useful in interpreting other observations; in particular, BPR and tide gauge measurements at other choke points where zonal coherence seems much higher to the south than to the north (P. L. Woodworth and T. Whitworth 1996, personal communication). This is to be investigated further as part of a joint analysis of all the WOCE choke point datasets. It would also be enlightening to further investigate these ideas using other wind stresses, for example, those from the ERS scatterometers. A potential problem with such a study is that the variability in the southern mode may be difficult to examine in satellite data due to the presence of sea ice. It is possible that the effect of sea ice on wind stress might account for some of the anomalous behavior seen at the annual period, although there are undoubtedly steric effects at the annual period due to the seasonal cycle of ice formation and melting. The high correlation between the POCM transports and measured pressures suggests that it will be worthwhile to use this and similar models to investigate the dynamics of these transport fluctuations in more detail.

Finally it is worth noting that, for the southern mode, it is misleading to speak of transport fluctuations in the ACC, for semiannual and shorter periods at least. The controlling dynamics, and therefore the path followed by the mean ACC, are different from those of the fluctuating current. If coherence around Antarctica can be established, the fluctuations should properly be termed fluctuations in Antarctic circumpolar transport.

Acknowledgments. The authors are grateful to Bob Spencer and the POL Technology Group for deploying and recovering the BPRs and calibrating the data. We are also indebted to Robin Tokmakian (Naval Postgraduate School, Monterey) for her time spent extracting and sending the relevant POCM data, to Tony Craig (NCAR) for supplying the gridded wind stress data, to the Permanent Service for Mean Sea Level at POL for Faraday sea levels, to William Connolley (BAS) for the Faraday atmospheric pressures, and to Phil Woodworth and Dave Stevens for useful discussions. This work was funded partly by the U.K. Defence Research Agency and the U.K. Natural Environment Research Council.

REFERENCES

Anderson, D. L. T., and A. E. Gill, 1975: Spin-up of a stratified ocean, with applications to upwelling. *Deep-Sea Res.,* **22,** 583–596.

——, and P. D. Killworth, 1977: Spin-up of a stratified ocean, with topography. *Deep-Sea Res.,* **24,** 709–732.

Baker, D. J., Jr., 1982: A note on Sverdrup balance in the southern ocean. *J. Mar. Res.,* **40**(Suppl.), 20–26.

Branstator, G., and J. D. Opsteegh, 1989: Free solutions of the barotropic vorticity equation. *J. Atmos. Sci.,* **46,** 1799–1814.

Bryden, H. L., and R. A. Heath, 1985: Energetic eddies at the northern edge of the Antarctic Circumpolar Current in the southwest Pacific. *Progress in Oceanography,* Vol. 14, Pergamon, 65–87.

Chelton, D. B., 1982: Statistical reliability and the seasonal cycle: Comments on ''Bottom pressure measurements across the Antarctic Circumpolar Current and their relation to the wind.'' *Deep-Sea Res.,* **29A,** 1381–1388.

——, A. M. Mestas-Nunez, and M. H. Freilich, 1990: Global wind stress and Sverdrup circulation from the Seasat scatterometer. *J. Phys. Oceanogr.,* **20,** 1175–1205.

Clarke, A. J., 1982: The dynamics of large-scale, wind-driven variations in the Antarctic Circumpolar Current. *J. Phys. Oceanogr.,* **12,** 1092–1105.

Dittmer, K., 1977: The hydrodynamic roughness of the sea surface at low wind speeds. *Meteor. Forschungsergeb.,* **12**(B), 10–15.

ECMWF, 1991: European Centre for Medium-Range Weather Forecasts model physical parameterisation. ECMWF Research Manual 3, 97 pp.

——, 1992: European Centre for Medium-Range Weather Forecasts data assimilation. ECMWF Research Manual 1, 82 pp.

FRAM Group, 1991: An eddy-resolving model of the Southern Ocean. *Eos, Trans. Amer. Geophys. Union,* **72**(17), 169–175.

Gill, A. E., 1968: A linear model of the Antarctic circumpolar current. *J. Fluid Mech.,* **32,** 465–488.

——, and P. P. Niiler, 1973: The theory of the seasonal variability in the ocean. *Deep-Sea Res.,* **20,** 141–177.

Grose, T. J., J. A. Johnson, and G. R. Bigg, 1995: A comparison between the FRAM (Fine Resolution Antarctic Model) results and observations in Drake Passage. *Deep-Sea Res.,* **42,** 365–388.

Han, Y. -J., and S. -W. Lee, 1981: A new analysis of monthly mean wind stress over the global ocean. Climatic Research Institute Rep. 26, 148 pp. [Available from Oregon State University, Corvallis, OR 97331-4501.]

Hellerman, S., and M. Rosenstein, 1983: Normal monthly wind stress over the world ocean with error estimates. *J. Phys. Oceanogr.,* **13,** 1093–1104.

Hughes, C. W., 1996: The use of topographic wave modes to solve for the barotropic mode of a rigid-lid ocean model. *J. Atmos. Oceanic Technol.,* **13,** 751–761.

——, 1997: Comments on ''On the obscurantist physics of 'form drag' in theorizing about the Circumpolar Current.'' *J. Phys. Oceanogr.,* **27,** 209–210.

——, and P. D. Killworth, 1995: Effects of bottom topography in the large-scale circulation of the Southern Ocean. *J. Phys. Oceanogr.,* **25,** 2485–2497.

——, M. S. Jones, and S. Carnochan, 1998: The use of transient features to identify eastward currents in the Southern Ocean. *J. Geophys. Res.,* **103,** 2929–2944.

Jayne, S. R., and R. Tokmakian, 1997: Forcing and sampling of ocean general circulation models: Impact of high-frequency motions. *J. Phys. Oceanogr.,* **27,** 1173–1179.

Johnson, G. C., and H. L. Bryden, 1989: On the size of the Antarctic Circumpolar Current. *Deep-Sea Res.,* **36,** 39–53.

Johnson, M. A., 1990: A source of variability in Drake Passage. *Contin. Shelf Res.,* **10,** 629–638.

Killworth, P. D., and M. M. Nanneh, 1994: Isopycnal momentum budget of the Antarctic Circumpolar Current in the Fine Resolution Antarctic Model. *J. Phys. Oceanogr.,* **24,** 1201–1223.

Klinck, J. M., 1991: Vorticity dynamics of seasonal variations of the Antarctic Circumpolar Current from a modeling study. *J. Phys. Oceanogr.,* **21,** 1515–1533.

Large, W. G., and S. Pond, 1982: Sensible and latent heat flux measurements over the oceans. *J. Phys. Oceanogr.,* **12,** 464–482.

Levitus, S., 1982: *Climatological Atlas of the World Ocean.* NOAA Prof. Paper No. 13, U. S. Govt. Printing Office, 173 pp.

Meredith, M. P., 1995: On the temporal variability of the transport through Drake Passage. Ph.D. thesis, University of East Anglia, Norwich, United Kingdom, 227 pp. [Available from University of East Anglia, Norwich NR4 7TJ, United Kingdom.]

——, J. M. Vassie, K. J. Heywood, and R. Spencer, 1996: On the temporal variability of the transport through Drake Passage. *J. Geophys. Res.,* **101,** 22 485–22 494.

——, ——, R. Spencer, and K. J. Heywood, 1997: On the processing and application of inverted echo sounder data from Drake Passage. *J. Atmos. Oceanic Technol.,* **14,** 871–882.

Morrow, R., R. Coleman, J. Church, and D. Chelton, 1994: Surface eddy momentum flux and velocity variances in the Southern Ocean from Geosat altimetry. *J. Phys. Oceanogr.,* **24,** 2050–2071.

Munk, W. H., and E. Palmén, 1951: Note on the dynamics of the Antarctic Circumpolar Current. *Tellus,* **3,** 53–55.

Olbers, D., 1998: Comments on ''On the obscurantist physics of 'form drag' in theorizing about the Circumpolar Current.'' *J. Phys. Oceanogr.,* **28,** 1647–1654.

Peterson, R. G., 1988a: On the transport of the Antarctic Circumpolar Current through Drake Passage and its relation to wind. *J. Geophys. Res.,* **93,** 13 993–14 004.

——, 1988b: Comparisons of sea level and bottom pressure measurements at Drake Passage. *J. Geophys Res.,* **93,** 12 439–12 448.

Read, P. L., P. B. Rhines, and A. A. White, 1986: Geostrophic scatter diagrams and potential vorticity dynamics. *J. Atmos. Sci.,* **43,** 3236–3240.

Schacher, G. E., K. L. Davidson, T. E. Houlihan, and C. W. Fairall, 1981: Measurements of the rate of dissipation of turbulent kinetic energy, ϵ, over the ocean. *Bound. Layer Meteor.,* **20,** 321–330.

Semtner, A. J., Jr., and R. M. Chervin, 1992: Ocean general circulation from a global eddy-resolving model. *J. Geophys. Res.,* **97,** 5493–5550.

Spencer, R., and J. M. Vassie, 1997: The evolution of deep ocean pressure measurements in the U.K. *Progress in Oceanography,* Vol. 40, Pergamon, 423–435.

——, and Coauthors, 1993: The ACCLAIM Programme in the South Atlantic and Southern Ocean. *Int. Hydrogr. Rev.,* **70,** 7–21.

Stammer, D., R. Tokmakian, A. Semtner, and C. Wunsch, 1996: How well does a ¼° global circulation model simulate large-scale oceanic observations? *J. Geophys. Res.,* **101,** 25 779–25 811.

Stevens, D. P., 1991: The open boundary condition in the United Kingdom Fine-Resolution Antarctic Model. *J. Phys. Oceanogr.,* **21,** 1494–1499.

——, and P. D. Killworth, 1992: The distribution of kinetic energy in the Southern Ocean. A comparison between observations and an eddy resolving general circulation model. *Philos. Trans. Roy. Soc. London,* **338B,** 251–257.

Stommel, H., 1957: A survey of ocean current theory. *Deep-Sea Res.,* **4,** 149–184.

Treguier, A. M., and J. C. McWilliams, 1990: Topographic influence on wind-driven stratified flow in a β-plane channel: An idealized model for the Antarctic Circumpolar Current. *J. Phys. Oceanogr.,* **20,** 321–343.

Trenberth, K. E., 1992: Global analyses from ECMWF and atlas of 1000 to 10mb circulation statistics. NCAR Tech. Note TN-373+STR, National Center for Atmospheric Research, Boulder, CO, 191 pp.

Warren, B. A., J. H. LaCasce, and P. E. Robbins, 1996: On the obscurantist physics of ''form drag'' in theorizing about the Circumpolar Current. *J. Phys. Oceanogr.,* **26,** 2297–2301.

——, ——, and ——, 1997: Reply. *J. Phys. Oceanogr.,* **27,** 211–212.

Wearn, R. B., and D. J. Baker Jr., 1980: Bottom pressure measurements across the Antarctic Circumpolar Current and their relation to the wind. *Deep-Sea Res.,* **27A,** 875–888.

Wells, N. C., and B. A. de Cuevas, 1995: Vorticity dynamics of the Southern Ocean from a general circulation model. *J. Phys. Oceanogr.,* **25,** 2569–2582.

Whitworth, T., III, 1983: Monitoring the transport of the Antarctic Circumpolar Current at Drake Passage. *J. Phys. Oceanogr.,* **13,** 2045–2057.

——, and R. G. Peterson, 1985: Volume transport of the Antarctic Circumpolar Current from bottom pressure measurements. *J. Phys. Oceanogr.,* **15,** 810–816.

——, W. D. Nowlin, and S. J. Worley, 1982: The net transport of the Antarctic Circumolar Current through Drake Passage. *J. Phys. Oceanogr.,* **12,** 960–970.

Willebrand, J., S. G. H. Philander, and R. C. Pacanowski, 1980: The oceanic response to large-scale atmospheric disturbances. *J. Phys. Oceanogr.,* **10,** 411–429.

Wolff, J. -O., E. Maier-Reimer, and D. Olbers, 1991: Wind-driven flow over topography in a zonal β-plane channel: A quasi-geostrophic model of the Antarctic Circumpolar Current. *J. Phys. Oceanogr.,* **21,** 236–264.

Woodworth, P. L., J. M. Vassie, C. W. Hughes, and M. P. Meredith, 1996: A test of the ability of TOPEX/POSEIDON to monitor flows through the Drake Passage. *J. Geophys. Res.,* **101,** 11 935–11 947.